UNIVERSITÀ DEGLI STUDI DI PADOVA

DIPARTIMENTO DI SCIENZE CHIMICHE

CORSO DI LAUREA MAGISTRALE IN CHIMICA

TESI DI LAUREA MAGISTRALE

AMINOLYSIS OF POLYURETHANE – BEYOND POLYOL RECOVERY

Relatore: Prof. Luca Dell'Amico

Correlatore: Prof. Troels Skrydstrup

Controrelatore: Prof. Marco Zecca

Laureanda: Chiara Sella

Nr. Matricola 2019467

Anno Accademico 2022/2023

1 TABLE OF CONTENTS:

2 ACKNOWLEDGMENTS

I extend my deepest gratitude to Prof. Dr. Troels Skrydstrup and Prof. Dr. Dell'Amico Luca for providing me with the invaluable opportunity to conduct my thesis project collaboratively between the University of Padua and the University of Aarhus, focusing on a subject dear to my heart.

I would like to express profound thanks to Assistant Professor Steffan Kvist Kristensen and Dr. Bjarke Skyum Donslund for their unwavering support, comprehensive guidance, and significant contributions to the development of my thesis. Their expertise and accessibility have not only enriched my cultural background but have also greatly enhanced the overall quality of my work.

The experience gained in Prof. Dr. Troels Skrydstrup's group was pivotal in shaping my understanding. I extend my sincere gratitude to all the people within this group for their exceptional availability and collaborative spirit, which profoundly influenced the entire project's experience.

3 ABSTRACT

As the global market for polyurethane continues to expand with an estimated projection to exceed 30 million tons by 2030, the volume of PU waste continues to rise. Unfortunately, landfilling remains the predominant disposal method due to the resistance of PU to various degradation factors and potential toxicity of combustion byproducts.

This study addresses the pressing need for technologies capable of depolymerizing PU, a task made challenging by its cross-linked polymeric structure and lack of a distinct melting point. Unlike thermoplastics, which already have established recycling processes, thermoset plastics like PU require specialized approaches.

This project focuses on achieving a comprehensive molecular recycle of PU, with particular emphasis on evaluating the aromatic fraction post-polyol filtration. Previous studies have predominantly centred on polyol fraction recovery, whereas this report shifts the focus towards identifying and decomposing aromatic hard segments for amine recovery. Initial aminolysis reactions were conducted to recover the polyol and to obtain the aromatic residue which was analysed, revealing the presence of urea functionalities. Furthermore, the aim was to complete the molecular recycling of the process and so the aromatic residue was subjected to further treatment. For this purpose, four different models were synthesized in order to study the decomposition reactions to recover diamines. The strategic selection of diamines, including TDA and MDA, precursor to TDI and MDI, streamlined the subsequent assessment of the aromatic fraction. Consequently, the resulting product after evaluation consists solely of one type of diamine, which can be readily employed for ongoing aminolysis or the reformation of isocyanate precursors.

6

4 ABBREVIATIONS

|			
Ar	Aryl	o/n	Overnight
Ac	Acetyl	PE	Polyethylene
ATR	Attenuated total reflection	PET	Polyethylene terephthalate
Bu	Butyl	Ph	Phenyl
DA	Diamine	ppm	Parts per million
DCM	Dichloromethane	PS	Polystyrene
DMSO	Dimethyl sulfoxide	PT	Para-toluidine
DTMAC	Dodecyltrimethylammonium chloride	PTC	Phase transfer catalyst
EoL	End-of-life	PTFE	Polytetrafluoroethylene
equiv.	Equivalent(s)	PU	Polyurethane
ESI	Electrospray ionization	PUF	Polyurethane foam
Et	Ethyl	TBAB	Tetrabutylammonium bromide
EDA	Ethylenediamine	TBAC	Tetrabutylammonium chloride
FT-IR	Fourier-transform infrared spectroscopy	TBAS	Tetrabutylammonium hydrogensulfate
HMDA	Hexamethylenediamine	TDA	Toluene diamine
HS	Hard segment	TDI	Toluene diisocyanate
m	Meta	Temp.	Temperature
MDA	Methylene dianiline	THF	Tetrahydrofuran
MDI	Methylene diphenyl diisocyanate	THTDPB	Trihexyl(tetradodecyl) phosphonium bromide
Me	Methyl	TLC	Thin-layer chromatography
MLC	Metal-ligand cooperation	TOAB	Tetraoctylammonium bromide
n.d.	Not determined	TOF	Time-of-flight
NMR	Nuclear magnetic resonance	UV	Ultraviolet
		wt%	Weight percent

5 INTRODUCTION:

5.1 POLYURETHANE OVERVIEW

Polyurethane, often abbreviated as PU, stands as one of the most versatile and widely used polymers in modern industry. Due to its adaptable nature, polyurethane finds application in an astonishing array of everyday products, ranging from footwear and furniture to refrigerators and freezers but also in advanced, high-end technologies like wind turbine blades, medical devices, and serves as essential components in both aircraft and spacecraft [1] (**Table 1**).

Table 1. General PU foam classification

PU foam nature	Applications
Flexible solid	Shoe sole, coating, adhesives
Flexible foamed	Cushioning, memory foam
Rigid solid	Turbine blades, medical devices, car body
Rigid foamed	Shock-absorption, insulation

This great potential for use in different applications is based on its structure-property relationships: it is synthesized through a process of polymerization known as polyaddition, involving the combination of diisocyanates and polyols. This reaction leads to the formation of polyurethane groups within the polymer's structure **(Figure 1)** [2] [3].

Figure 1: General polymerization process of PU
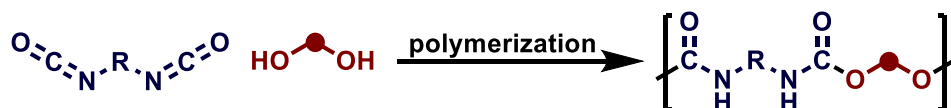
During the synthesis of this highly employed plastic some additives are usually added such as blowing agents that during the foaming process expand the foam, and surfactants which stabilize and control the size of the

pores and the dispersity of the air bubbles into the foam. [3] The nature of polyol and diisocyanate deeply influence the properties of the final PU. Diols with lower molecular weight results in the formation of rigid, brittle polymers, primarily due to the higher concentration of polyurethane, on the other hand, when employing long-chain polyols with lower functionality (indicating fewer OH groups), the resulting polyurethane exhibits a softer and more elastic quality (**Figure 2**). Furthermore, a higher functionality, denoting a greater number of OH groups, facilitates cross-linking within the polyurethane structure, imparting additional strength and resilience [4][3].

**Figure 2: Small selection of polyols employed in PU production**
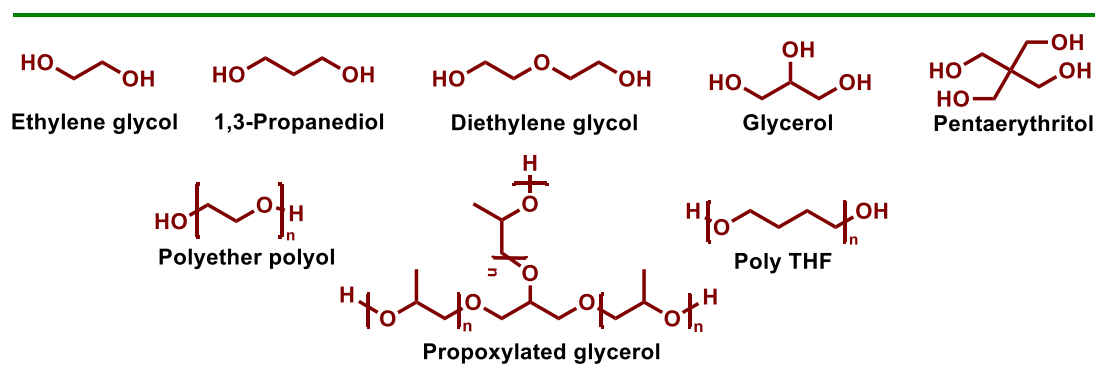
On the other hand the nature of isocyanate plays distinct roles in the hardness and stability of PU. For instance, aromatic diisocyanates, which exhibit notably higher reactivity compared to their aliphatic or cycloaliphatic counterparts, yield PU formulations with greater rigidity as opposed to aliphatic variants [4]. Among the aromatic diisocyanates, those with the highest technical significance include TDI, comprising the isomers 2,4-TDI and 2,6-TDI, and methylene diphenyl diisocyanate (MDI), which includes 4,4'-MDI and 2,4'-MDI as illustrated in **Figure 3** [2].

Figure 3: Small section of diisocyanates employed in PU production
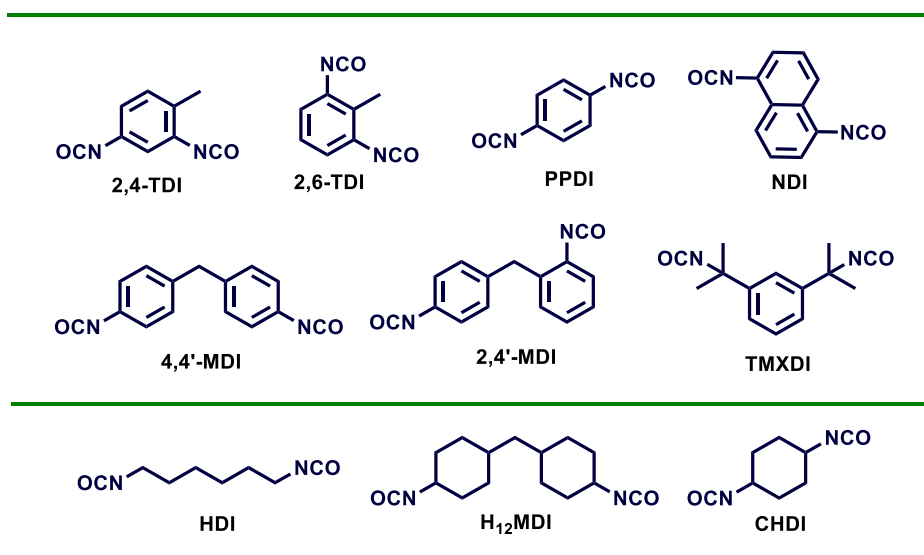
Both these two main reagents are obtained from fossil fuels sources through industrial process that are economically advantageous but environmentally not sustainable [5]. The most widely used way to produce isocyanates is through the reaction of phosgene with amines. Even if phosgene is known for being a highly toxic gas and its reaction is harmful to human and animal health [5] it is highly employed in the production of isocyanate . For the general production of polyol the precursor have petrochemical sources [6]. (**Scheme 1**)
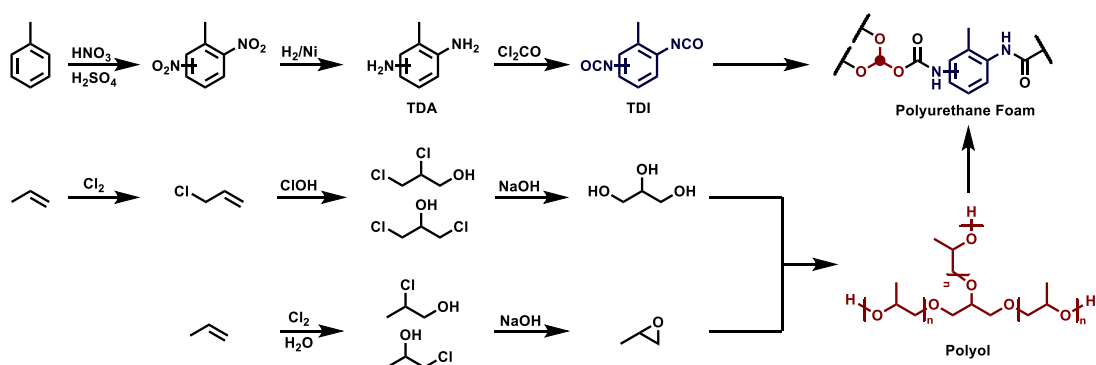

Scheme 1: Example of a production of polyurethane foam from platform molecules.

In the last few years the depletion of fossil fuels has influenced the production of these polymers precursor. One of the solution that is still developing is the employment of bio-based chemicals: polyols from vegetable oil, lignin, and carbohydrates are already obtained through

processes of epoxidation, hydroformylation and transesterification even if molecular complexity of biomass composition make it challenging [7]. Moreover, replacing petrochemical isocyanates with their bio-based alternatives is not so obvious but it is feasible, and there are ongoing researches and development in the field [5]. Nonetheless, at the moment these new synthetic pathways to bio-based isocyanates still require phosgene as a petroleum-based reagent [7]. Some bio-based PUs were synthesized but the properties of them are still not comparable to the petroleum-based PUs, moreover from the economical point of view these processes are more expensive for several reasons such as the necessity of technological development and the feedstock cost [5].

Concurrently with these cutting-edge production technologies, numerous studies are underway regarding the disposal and depolymerization of this material. Sure enough, as can be deduced from its huge versatility, the global market of PU continues to grow and has exceeded 25 million metric tons as of 2021. The production is estimated to surpass 30 million tons by 2030 (**Figure 4**) [8].

Figure 4: Market volume of PU worldwide from 2015 to 2022, with a forecast for 2023 to 2030 (in million metric tons) [8]
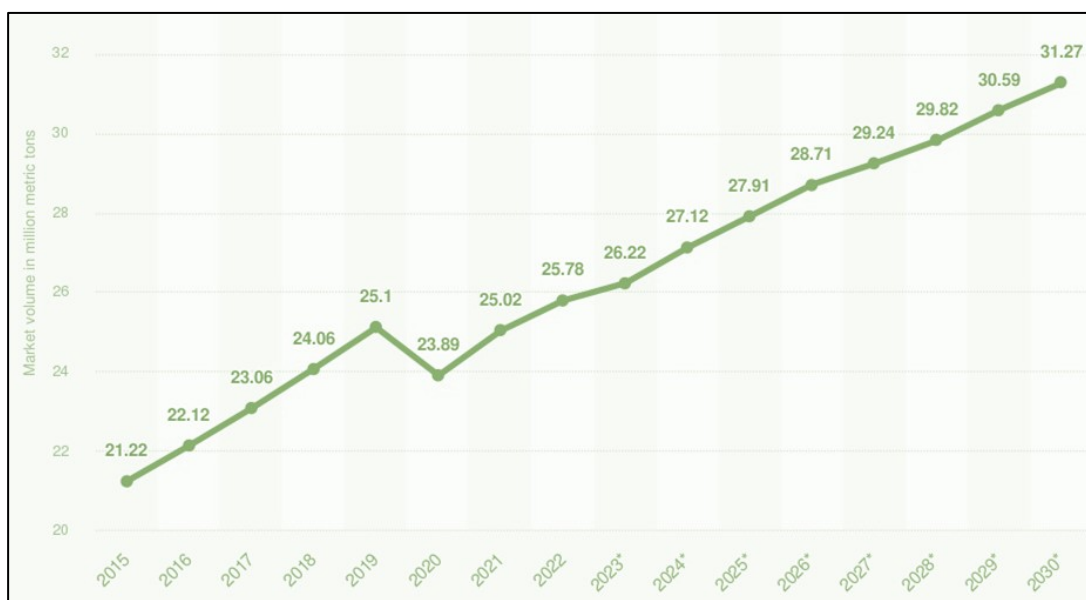
According to these numbers, it is not unexpected that the volume of PU waste continues to rise annually. Regrettably, landfilling remains the

predominant method of disposal due to its resistance to various physical, chemical, and biological factors, as well as the potential toxicity of certain combustion byproducts, which often hinder alternative waste management approaches [9].

The urgency for technologies capable of depolymerizing this polymer is evident. However, in comparison to thermoplastics like PE, PET, and PS, which already have established functional recycling processes, they have fallen behind [9] [10]. The key distinction in recyclability lies in the chemical composition of thermoplastics and thermoset plastics. The former can be melted and moulded into new products, allowing for a certain degree of recycling. In contrast, the latter consist of a cross-linked polymeric structure without a distinct melting point, precluding similar recycling strategies as those applicable to thermoplastic materials [10].
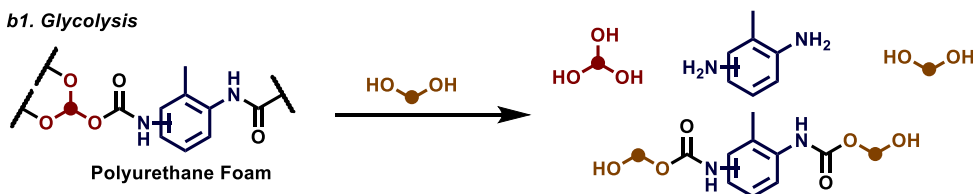
5.2 DEPOLYMERIZATION PROCESSES

A range of chemical recycling technologies, including glycolysis, acidolysis, hydrolysis, aminolysis, and catalytic hydrogenation, have been explored for the disassembly of PU materials [11].
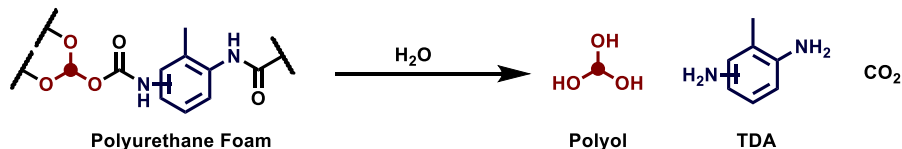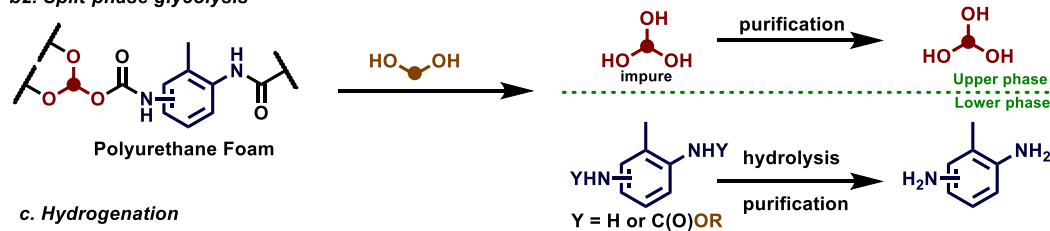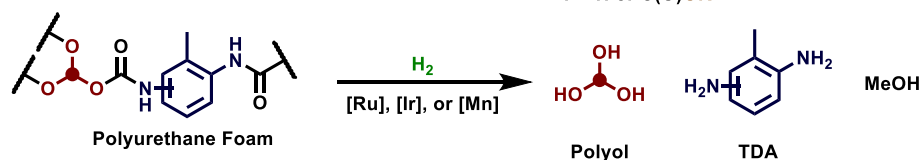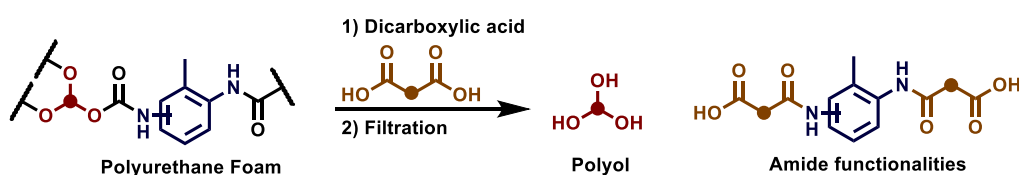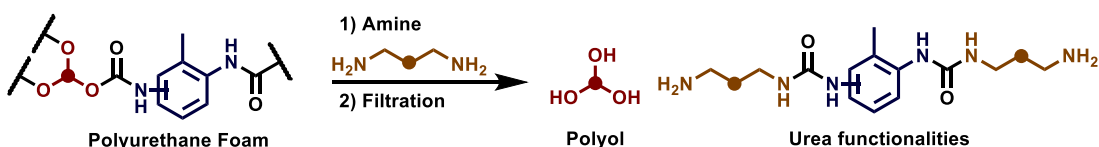

Scheme 2: Chemical recycling technologies for deconstruction of polyurethane. Adapted from [11]

Hydrolysis, the initial chemical method developed for recycling polyurethane waste, especially flexible foams, involves a reaction between polyurethane waste and either liquid or steam water (**Scheme 2, a**). This process yields polyols, amine intermediates, and carbon dioxide. It occurs in an anaerobic environment at high temperatures (above 150–320 °C). The resulting polyols can be used as additives in original polyol for polyurethane and other polymers production. Additionally, treating amine intermediates with phosgene allows for the recovery of the initial isocyanates. [12] However, a notable drawback is the high energy input required to either heat up the batch full of water or apply high pressure in the reactor, making this process economically challenging. [9] [12] Due to this reason, hydrolysis has found industrial adoption just recently.

Conversely, glycolysis processes hold historical significance, having been initially employed for recovering polyol from PET. This same procedure was subsequently adapted and tested with PU substrates, yielding results that demonstrated compatibility with both flexible and rigid foam. [13] Traditional glycolysis involves heating PU foam in a diol like diethylene glycol or diglycerol, with or without catalyst, yielding a mixture of residual diol, polyol, dianiline, and related compounds (**Scheme 2, b1**). To address the presence of unwanted aromatic amines, they are converted into nonvirgin polyols, albeit resulting in a mixture necessitating the addition of a significant amount of virgin polyol for foam reformulation. This traditional process underwent refinement with the advent of split-phase glycolysis, (**Scheme 2, b2**) which introduces a nuanced approach. It separates the post-reaction mixture into two distinct phases: the upper phase, rich in polyol, undergoes additional refinement to yield a pure polyol fraction. Meanwhile, the lower phase undergoes hydrolysis to isolate dianilines, along with diglycerol and catalysts. While split-phase glycolysis primarily focuses on original polyols and dianilines, further refinement steps are essential for complete isolation. [13] [11]

Recently, the combination of transition metal catalysts and hydrogen has been applied to PU substrates. (**Scheme 2, c**) This process represents an atom-efficient means for the deconstruction of the polymer, it circumvents the use of high-boiling glycol solvents but relies on expensive metal and ligand combinations. [10] In the last few years the groups of Milstein and Schaub reported the first examples of a transition metal-catalyzed hydrogenation of

PU with a Ru-based catalyst [14] [15] followed by the work of Skrydstrup and co-workers applying an iridium catalyst, later, Mn-based catalysts were disclosed being applicable as well [10] [16].

The last two reported methods are acidolysis and aminolysis, (**Scheme 2, d e)** both of which offer the benefit of producing a liquid polyol and a solid residue from the PU hard segments, allowing for the valuable polyol to be recovered through filtration [17] [18]. In the acidolysis process, the degrading agents, usually dicarboxylic acids like adipic acid, are applied in a slight excess to form thermodynamically stable amide bonds while the polyol is being recovered [18]. In the aminolysis process, amines and diamines react to form stable urea substances that can be separated from the polyol phase through filtration.

At the moment, this is the easiest way to recover the polyol in high purity concentrations so, for this reason, these two processes are more interesting from an industrial perspective. For both processes, it appears evident that after the polyol separation, a significant aromatic fraction will be discharged. Consequently, developing a method that converts the solid waste residue back into the starting diamine will facilitate a closed cycle in the depolymerization of PU.

This project aims to achieve a comprehensive molecular recycle of PU focusing on the evaluation of the aromatic fraction after the polyol filtration. While past studies primarily emphasized polyol fraction recovery, this report shifts the focus towards identifying and decompose the aromatic hard segments into amines which can be further converted to PU precursors. Initial aminolysis reactions were conducted (**Figure 5, 1)** to analyse the residue's composition, which, as anticipated, revealed the presence of urea functionalities. Furthermore, models were synthesized (**Figure 5, 2)** to facilitate the evaluation of reactions for recovering diamines. Consequently, the selection of diamines was strategically made to streamline the subsequent assessment of the aromatic fraction. Indeed, not only linear diamines were tested for the aminolysis but also TDA and MDA which are the precursor of TDI and MDI. This decision was made to eliminate the need for separating various diamines (**Figure 5, 3a)**. Consequently, the resulting product after evaluation consists solely of one type of diamine (**Figure 5, 3b)** which can be readily utilized for the ongoing aminolysis of new PU material or for the reformation of isocyanate precursors.

Figure 5: General scheme of the followed project

16
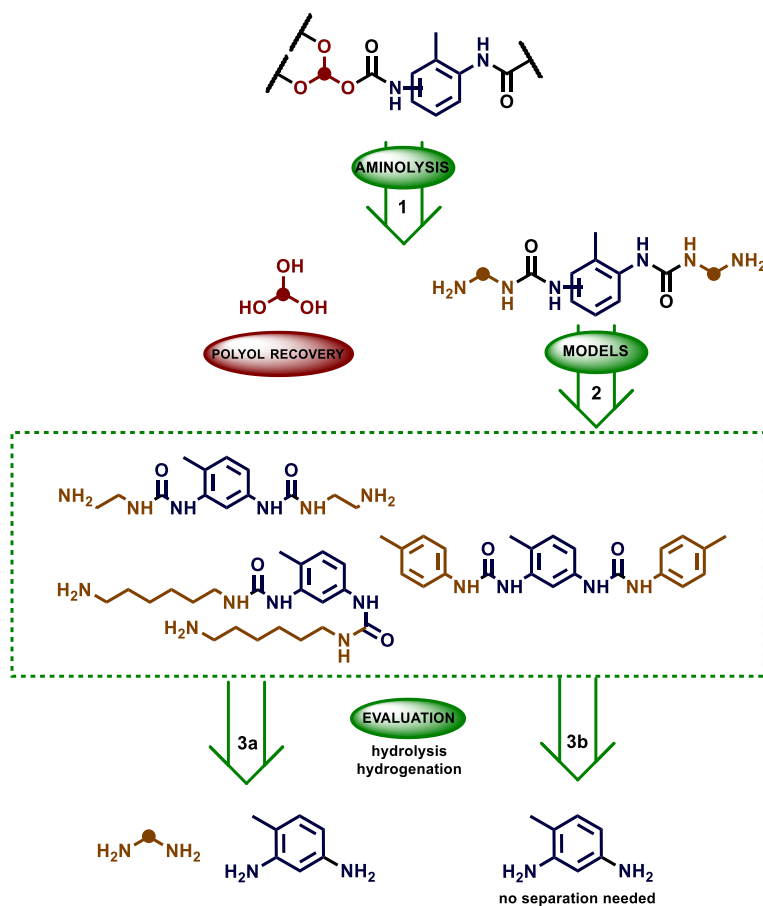
6 THEORETICAL BACKGROUND

6.1 UREA STABILITY

To conduct a thorough evaluation of the aromatic fraction, our attention must be directed towards the formation of urea bonds. The amide bond within the urea structure exhibits exceptional stability, owing to the conjugation effects between the lone electron pair on the nitrogen atom and the π-electrons on the carbonyl p-orbital (**Figure 6**). Additionally, the oxygen atom within the carbonyl group serves as a hydrogen bond acceptor, while the hydrogen atoms on the nitrogen atoms act as hydrogen bond donors [19].

Figure 6: Resonance structures of urea
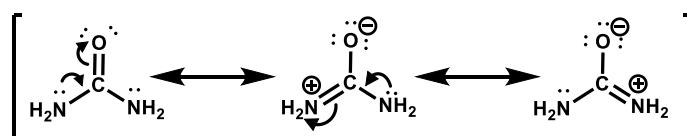
The derivatives of urea present this structural motif which finds versatile applications across various fields, including polymer production, creation of supramolecular systems and as protecting group [20]. The latter one is particularly relevant since urea functional group generally require harsh conditions for reactions with alcohols, amines, and thiols. While this characteristic renders them robust protecting groups for aromatic and aliphatic amines, it somewhat limits its subsequent cleavage.

Generally, the decomposition of urea functionalities proves to be a challenge since they have high stability, indeed they demand specific conditions such as acidic or basic environments or the presence of metal catalysts [21]. However, an intriguing equilibrium at relatively low temperatures may facilitate this process, in fact the system reaches equilibrium with isocyanates and amines, a reaction that becomes more favorable as the nitrogen atom gains greater substitution [20].

6.2 Hydrolysis

Considering the equilibrium presented in the previous paragraph, hydrolysis at high temperatures is more likely to occur through attack on the carbonyl carbon of the isocyanate in equilibrium with the initial model than a direct nucleophilic attack on the carbonyl carbon of urea. This attack has the potential to irreversibly shift the equilibrium towards favouring the dissociation reaction, ultimately resulting in the irreversible and complete degradation of the urea functionality (**Scheme 3**) [22].
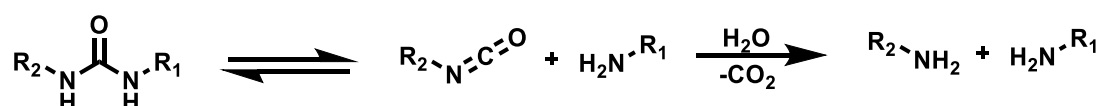

Scheme 3: Equilibrium of urea derivative at elevated temperature and consequent hydrolysis of isocyanate

While this equilibrium has long been recognized, it has garnered increased attention in recent years due to the growing need for hydrolysable materials that, thanks to the dynamic nature of the bonds such as urea bond, undergo a more straightforward recycling process [20]. For instance, Liu *et al*. successfully applied this process to achieve a more sustainable degradation of urea-formaldehyde resin residues. Typically, these residues necessitate combustion or pyrolysis for thermal evaluation, but both methods are inadequate for safe disposal due to the formation of nitrogen-containing gases such as ammonia, isocyanic acid, and hydrocyanic acid. The development of hydrothermal cleavage at temperatures below 140 °C resulted in complete decomposition without the release of harmful gases into the environment [23].

Moreover, Medina-Ramos *et al.* showed that water at elevated temperature (*WET*) [24] which exhibits substantially different physiochemical properties, as shown in several studies [25], can be employed for a wide range of synthetic transformations. Specifically, they studied the hydrolysis of N-*boc* (**Scheme**

4, a), during which a diarylureas intermediate was observed (**Scheme 4, b**). Over the course of the reaction, this intermediate exhibited a decreasing concentration, prompting considerations of its hydrolysis and subsequent formation of the corresponding anilines (**Scheme 4, c**) [24].
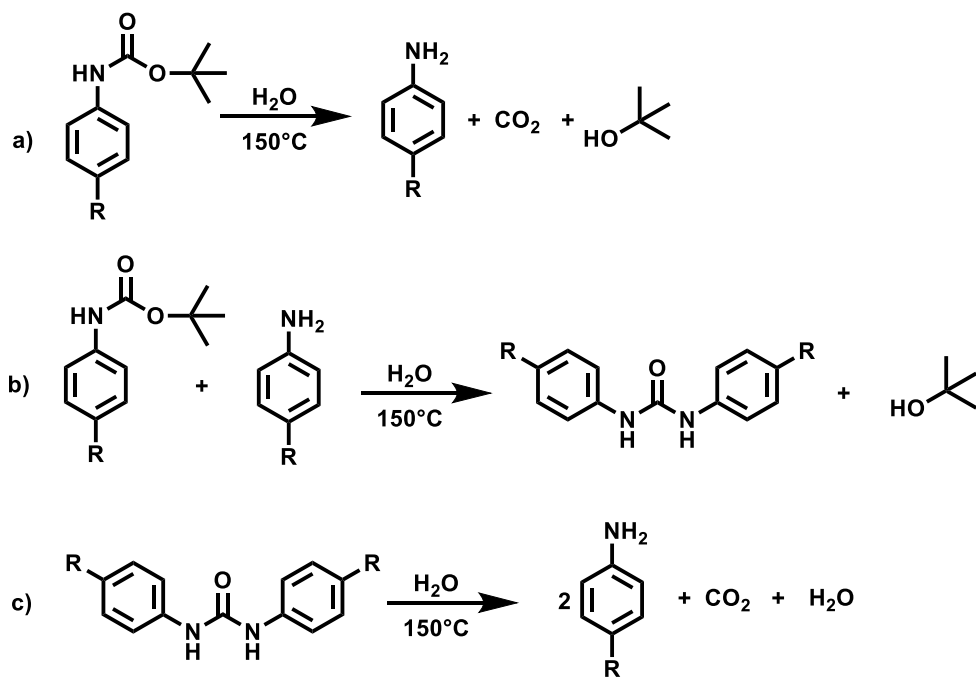

Scheme 4: WET hydrolysis of N-*Boc* group, adapted from reference [24].

6.3 HYDROGENATION

Catalytic hydrogenation of polar bonds, particularly carbonyl groups, provides an environmentally friendly pathway to synthesize important organic building blocks like alcohols and amines [26]. Ureas are notably challenging carbonyl compounds to hydrogenate, in fact, urea derivatives have been employed as solvents for hydrogenation reactions due to their unreactive nature toward hydrogenation [27]. The lower electrophilicity of the carbonyl group, due to resonance effects involving alkoxy or amido groups, could explain the difficulties to hydrogenate these substrates.

The general hydrogenation process of a carbonyl compound requires the cooperation between the metal centre and the ligand. This kind of cooperation is known as metal-ligand cooperation (MLC) and it foresees bond activation across both metal and ligand resembling oxidative addition and reductive elimination [28]. This process can be schematized in three steps (**Scheme 5**) where in the first we have the activation of the catalyst through MLC with molecular hydrogen, in the second we have the coordination of the carbonyl and in the end the hydride transfer which reduces the substrate and reforms the non-active catalyst form.
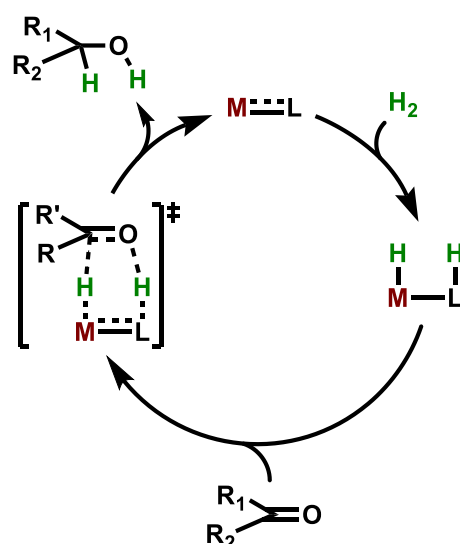
Scheme 5: Simplified catalytic cycle for hydrogenation of carbonyl bond, activation by MLC.
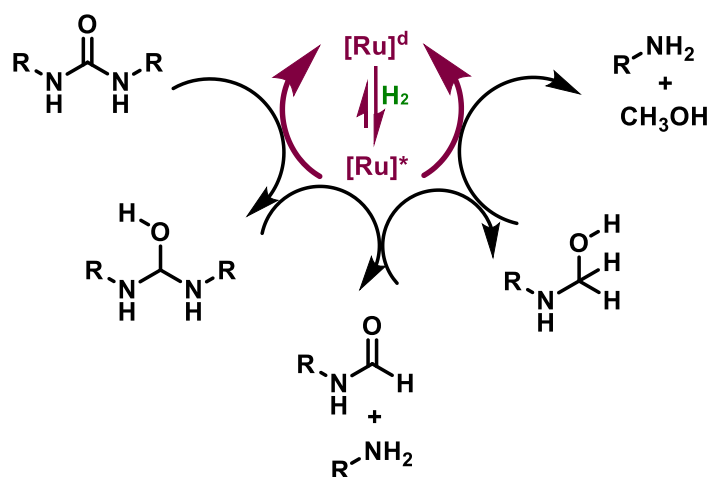
For the hydrogenation of urea derivatives the first catalyst employed was synthesized by Milstein and coworkers [29]. Here, they have developed a PNN and PNP Ru(II) pincer complexes based on pyridine and acridine backbones that provided the activation of the centre through a new mode of MLC, based on ligand aromatization-dearomatization. [29]

Ru-^{iPr}PNN precatalyst **[Ru]**   Ru-^{iPr}PNN dearomatized **[Ru]^d**   Ru-^{iPr}PNN active **[Ru]***
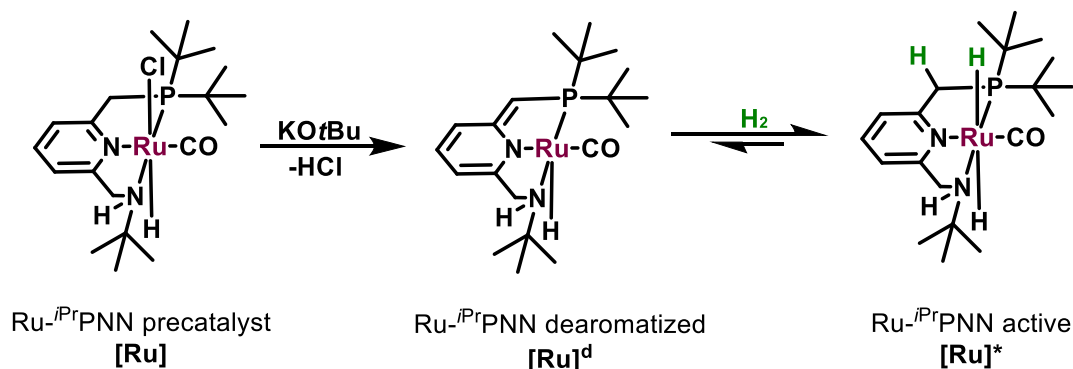
**Scheme 6: Activation of Ru-^{iPr}PNN catalyst by ligand aromatization-dearomatization**

The deprotonation of the benzylic α-proton to the pyridine group of Ru-^{iPr}PNN pre catalyst **[Ru]** by KO*t*Bu can lead to its de-aromatization (Ru-^{iPr}PNN dearomatized **[Ru]^d**) and so the moiety can regain its aromaticity by cooperation between the metal and the ligand, giving the activation of the catalyst when hydrogenation of it occurs (Ru-^{iPr}PNN active **[Ru]***) [30]. When the catalyst was studied by X-ray analysis, a shorter distance between the methylene carbon and the pyridinic carbon in one of the two arms of the ligand was revealed. This finding confirmed the occurrence of the process of dearomatization (**Scheme 6**) [31].

Initially, this catalyst was utilized to hydrogenate amide substrates but then also hydrogenation reaction of urea derivatives resulted in successful outcome. At 130° C in THF with Ru-^{iPr}PNN at 3 mol% and base at 4 mol% with 20 bar of H$_2$ they were able to convert it in amine and methanol with yields above 80%. During the analysis the observed formamide as intermediate underlined the suggest of a stepwise hydrogenation reaction, in which a formamide along with one equivalent of amine is initially formed by the cleavage of a C=N bond, followed by fast hydrogenation of the formamide, which does not accumulate (**Scheme 7**) [29].

Scheme 7: Presumed mechanism of Ru-^{iPr}PNN catalyst with ureic substrates

Another interesting study was reported by Kumar *et al.* which were able to hydrogenate a wide range of urea derivatives under the catalytic combination of 2 mol% of Ir-^{iPr}MACHO, 4 mol% KO*t*Bu under 50 bar of H$_2$ at 130°C for 24 hours [32] (**Scheme 8**).
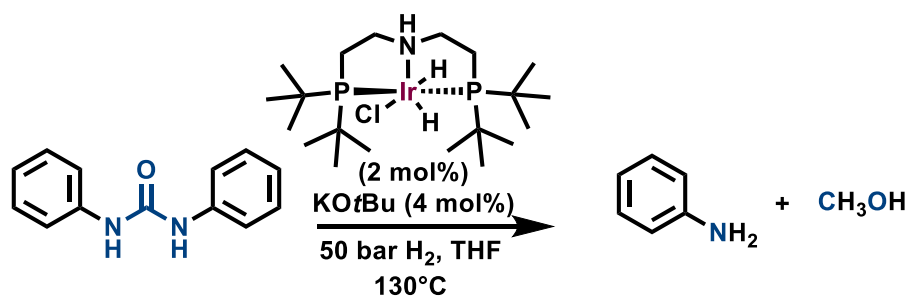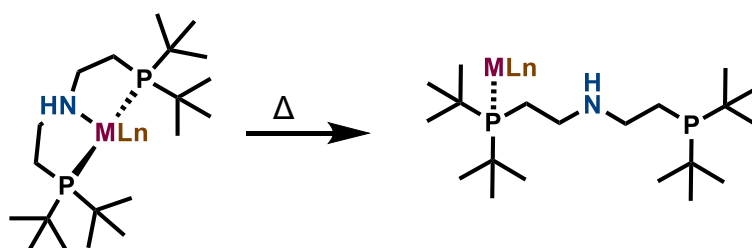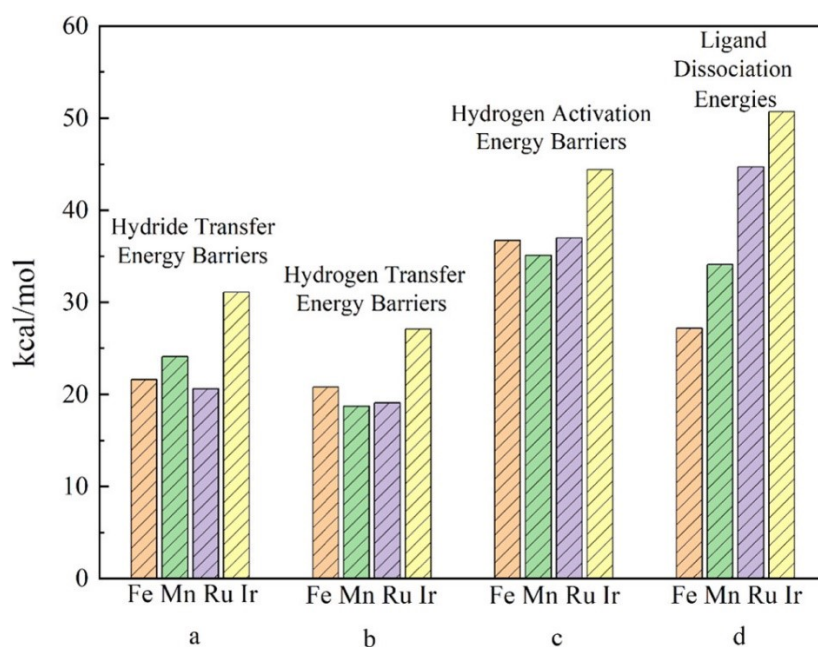

Scheme 8: Hydrogenation of urea derivative with Ir-MACHO catalyst in THF, 85% yield in aniline

During the process, the catalyst is activated by the base through MLC, and a stepwise proceeding is presumed. The MACHO complex has already been utilized in the hydrogenation of polyurethane, demonstrating successful conversion of PU to amine and polyol [10]. Due to the significance of this reaction, a more deep study was conducted focusing on changing the metal centre to perform the same reaction with a more earth-abundant metal. For this reason, Fe and Mn were complexed with the MACHO ligand, however, when the catalyst was applied to a PU sample, the reaction showed a lower yield in amine conversion [33].

From DFT calculations of the hydrogenation of phenylcarbamate using the wB97X-D method with def2-TZVPP basis sets, they were able to obtain the energy barrier values for hydride transfer, hydrogen transfer, and hydrogen activation. These values were lower for Mn compared to Ir, indicating that a higher activity should be expected for the Mn catalyst (**Figure 7**). In the same study, it was hypothesized that the difference could be explained through the dissociation of the pincer ligand from the metal centres. The ligand dissociation energies support this hypothesis: for Mn, Ru, and Ir catalysts, the values are 34.1, 44.7, and 50.7 kcal/mol, respectively [33]. (**Scheme 9**)

Figure 7: Trend of energy barriers when metal centre is changed. Adapted from [33]

**Scheme 9: Dissociation of MACHO ligand when the system reaches high temperatures**

Another pertinent hydrogenation process of urea derivatives was carried out in the presence of 2 mol% manganese [Ph2]PNP complexes and 6 mol% of KO*t*Bu in *i*PrOH, a solvent commonly used in transfer hydrogenation

reactions, also serving as a hydrogen donor. Under standard reaction conditions, symmetrically substituted urea derivatives were converted to the desired amines, yielding up to 91%, and methanol, yielding up to 89% [34] (**Scheme 10**). The significance of this study lies in the investigation of the kinetic profile, where the yield of carbamate during the reaction was monitored. The researchers observed a maximum of 71% after 2.5 hours, followed by a decrease in its concentration as the corresponding amine and methanol increased. These results suggest that carbamate is most likely a reaction intermediate in the transfer hydrogenation of urea derivatives [34].
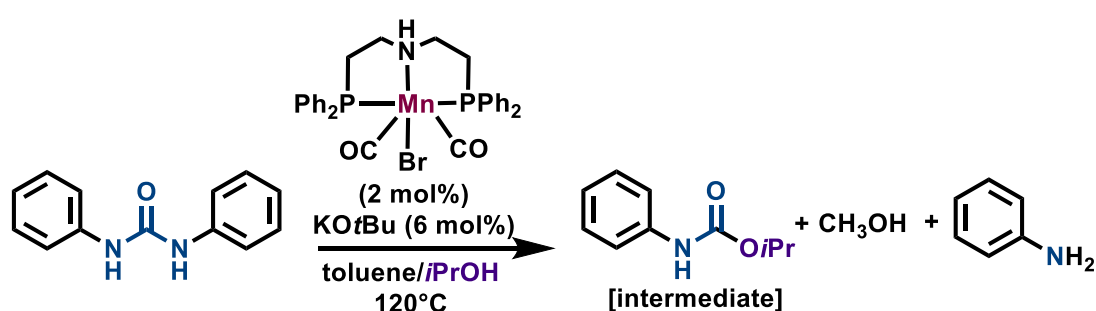
Scheme 10: Hydrogenation of urea derivative with Mn-PNP catalyst in *i*PrOH, formation of carbamate as intermediate

In the same study it is also proposed a catalytic cycle that is reported in **Scheme 11**. The initial formation of carbamate **4a** from the urea derivative **1a** and *i*PrOH is demonstrated to be a catalytic process with KO*t*Bu as catalyst. The sequence initiates with the deprotonation of the pre-catalyst Mn-IV by KO*t*Bu resulting in the formation of complex Mn-IV-1. Subsequently, dehydrogenation of *i*PrOH by Mn-IV-1 leads to complex Mn-IV-2 which is the active specie able to transfer the hydrogen to C=O group of carbamate intermediate **4a** furnishing Mn-IV-3. The elimination of *i*PrOH from Mn-IV-3, facilitated by metal-ligand cooperation, produces M-IV-4. Catalyst regeneration occurs through the release of formamide **5a**, which reverts to catalyst Mn-IV-1. The reaction of **5a** with Mn-IV-2 leads to the formation of complex Mn-IV-5, initiating the elimination of the final amine **2a**, and Mn-IV-6. Finally, formaldehyde **6a** undergoes reduction to yield methanol **3a**.
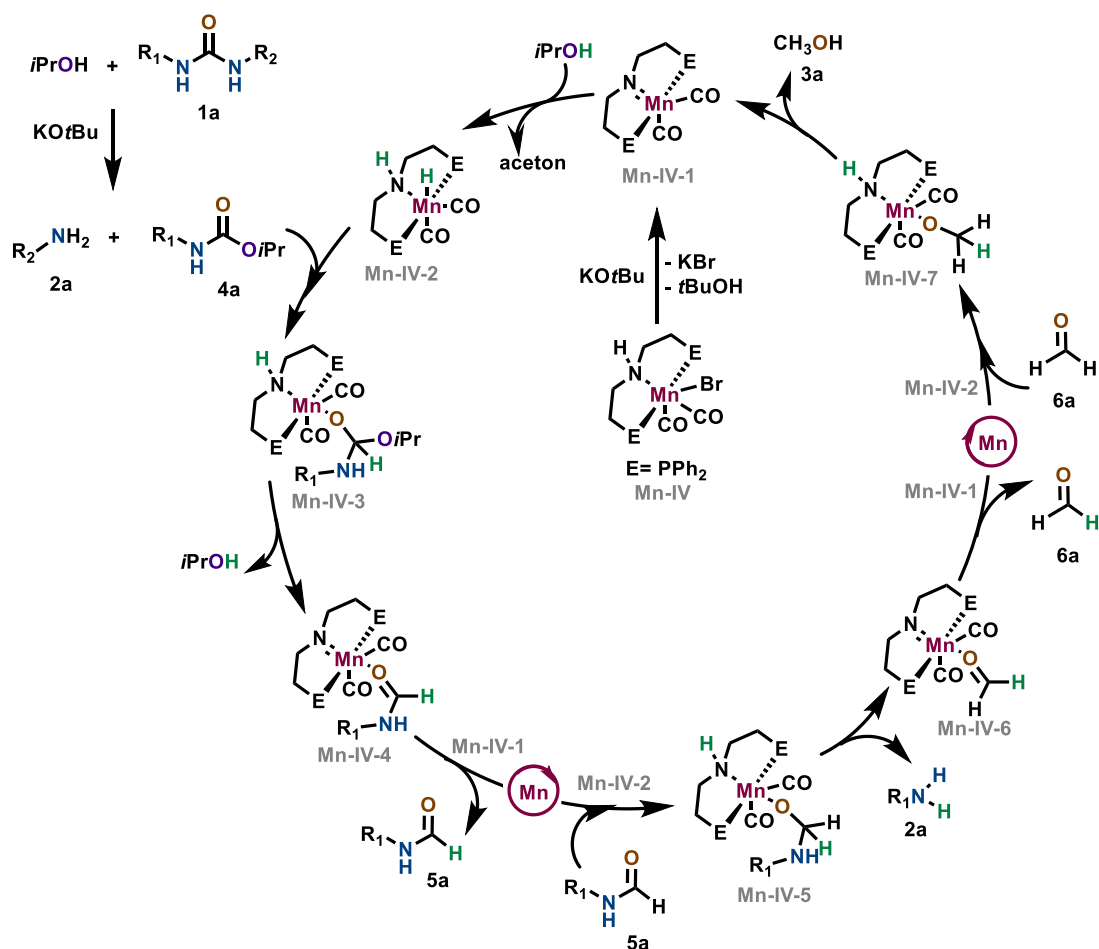
Scheme 11: Proposed reaction pathway for Mn-catalyzed hydronation of urea functionalities. Adapted from reference [34].

This study emphasizes the significance of the chosen solvent. It not only serves to dissolve the reagents, but also possesses various properties that can significantly impact catalysed reactions. A solvent can potentially interact with or react with a starting material, either activating or deactivating it for the reaction. Additionally, it may engage with a substrate, giving rise to a new intermediate that undergoes more (or less) selective transformation through catalysis [35].

# 7 RESULT AND DISCUSSION:

7.1 AMINOLYSIS:

The aminolysis tests were done on samples already characterized from previous studies. In accordance the previously reported methods the chosen foams derived from an EoL mattress and shoe sole, the first one was prepared by shredding on a modified twin screw extruder [36] while the second with a cutting mill fitted with a 1 mm filter [10].

The amount of diamine added was determined based on the composition of the respective samples. Considering the moles of TDI that are present in the pattern of PU (0.35 mmol in 260 mg of sample) and the moles of MDI present in the shoe sole (0.22 mmol in 260 mg of sample), 2.1 equivalents of diamines were added, one equivalent for each isocyanate functional group. During the aminolysis reaction, the amines undergo a reaction with the carbonyl carbon of the urethane bonds, leading to the liberation of the polyol and the formation of a residual ureic fraction that retains chemically useful bonds.

To confirm the purity of the extracted polyol, its ^{1}H-NMR spectra was compared with those of the polyol obtained from hydrogenation of the same PU flexible foam sample and PU shoe sole [10]. In accordance with the preceding investigation, wherein the polyol was subjected to characterization through MALDI-TOF analysis, determination of its structural attributes was achieved for both samples: for EoL PU flexible foam (**Figure 8a**) and for the one from PU shoe sole (**Figure 8c**). From this point onward, the respective simplified representations shown in **Figures 8b** and **8d** will be presented.

Figure 8: General motif of polyols:


- from PU flexible foam
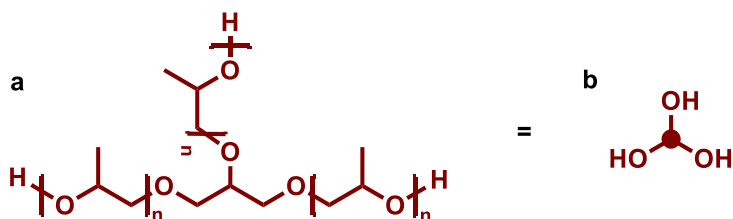
- from PU shoe sole
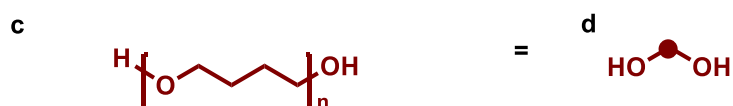
Initially, a set of screening reactions were conducted on 250 mg of flexible foam PU mattress in 8 mL vials using different diamines at 150 °C (see experimental section for full details, **10.1.5**). Here, using ethylenediamine (EDA) yielded a 35% polyol recovery while using 2,4-TDA resulted in a 55% recovery of the polyol (**Table 2**, entries 1 and 2). In an effort to increase the polyol yield, the equivalents of 2,4-TDA was increased. However, this did not lead to any improvement (**Table 2**, entry 3), as unreacted 2,4-TDA was detected and subsequently removed from the polyol fraction. No reactivity was observed even after 3-hours reaction time (**Table 2,** entry 4).

**Table 2. Aminolysis of PU Flexible Foam – 250 milligrams scale[a]**
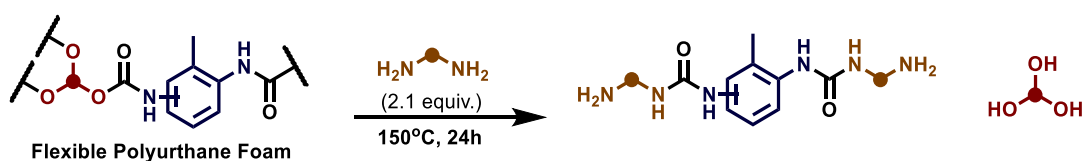
entry	DA	Polyol [mg]	Polyol [%][b]	Aromatic fraction [mg]	Change of reaction conditions
1	EDA	63	35	235	100°C
2	2,4-TDA	93	55	117	-
3	2,4-TDA	83	49	116	4 equiv. DA
4	2,4-TDA	n.d.	-	n.d.	3 hours

[a] Reactions performed as described in General Procedure 10.1.5. [b] Isolated yield. (DA diamine, EDA ethylendiamine, TDA toulendiamine)

In dealing with the vast amount of PU waste present, the scale of the reaction needed to be addressed. As such, the reaction scale was increased to 2 g of flexible foam. Unfortunately, upon scaling the reactions to 2 grams, the yields obtained from the 250 mg scale could not be maintained. Here, the reaction with EDA resulted in a 20% yield of polyol (**Table 3,** entry 1), accompanied by an aromatic residue that did not exhibit a repetitive structure. The residue had low solubility even in DMSO and contained a significant amount of polyol, even after five extractions with cyclohexane, indicating an incomplete aminolysis reaction. The reaction with hexamethylenediamine HMDA yielded a 73% polyol recovery (**Table 3,** entry 2) that necessitated acidic work-up for removing residual diamine to obtain a pure polyol. From NMR analysis it was possible to determine the composition of the aromatic fraction that yielded the expected 1,1'-(4-methyl-1,3-phenylene)bis(3-(6-aminohexyl)urea) and 1,1'-(2-methyl-1,3-phenylene)bis(3-(6-aminohexyl)urea) in a 4:1 ratio (**Figure 9a**), consistent with the regioisomeric composition of the starting PU material (4 : 1; 2,4-TDI : 2,6-TDI). During the identification of these two main products reported in **Figure 9a**, it was also possible to detect another five tolyl peaks in the region between 1.7 and 2.2 ppm, indicating the presence of other intermediates that were attributed to a partially aminolyzed fraction where polyol was still bonded to urethane bonds (**Figure 9b)**.

Table 3. Aminolysis of PU Flexible Foam with linear DA – 2 grams scale[a]

Flexible Polyurethane Foam
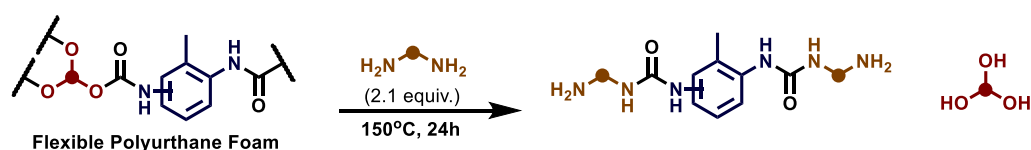
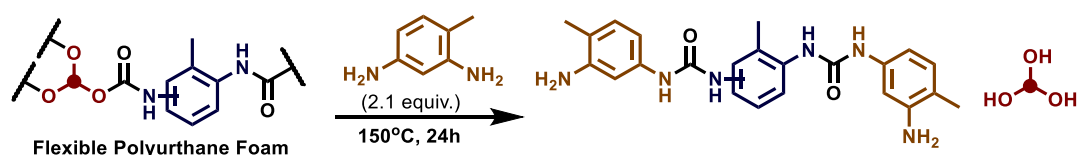| entry	DA	Polyol [mg]	Polyol [%][b]	Aromatic fraction [mg]	Change of reaction conditions
1	EDA	250	20	2058	100 °C [c]
2	HMDA	993	73	1022	-

[a] Reactions performed as described in General Procedure 10.1.5. [b] Isolated yield. [c] To avoid the boiling point of EDA (b.p. 116°C). (DA diamine, EDA ethylendiamine, HMDA hexamethyenediamine)

Figure 9: Desired products (a) and intermediates (b) of PU aminolysis with HMDA
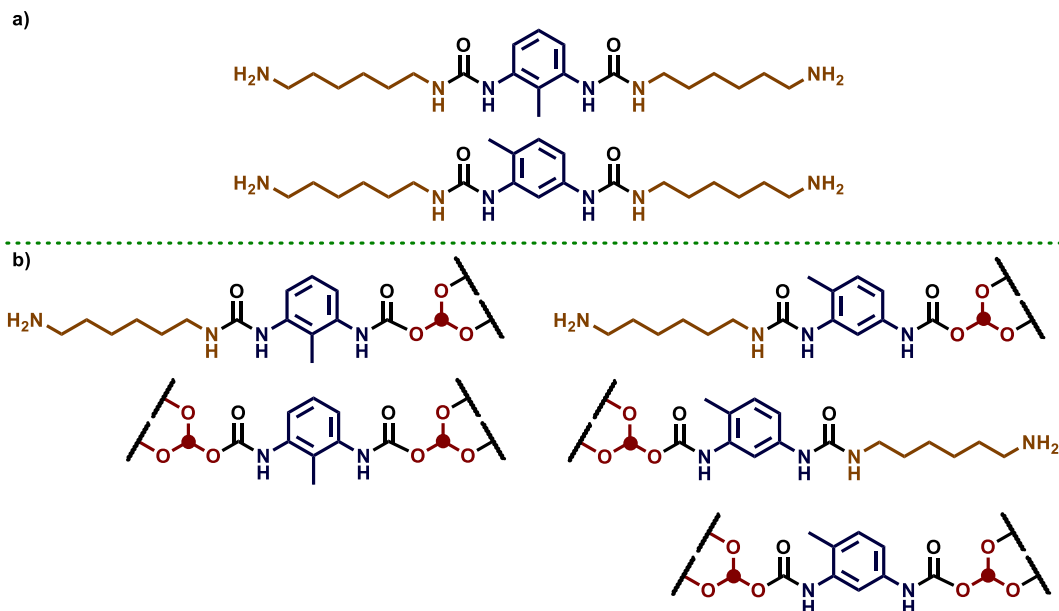
When the reaction was scaled-up using 2,4-TDA as degrading agent, the polyol yield was half of that obtained at 250 mg scale, (**Table 4**, entry 1). Consequently, knowing the central role of temperature for this reaction [37] [38] a COtube reactor was employed (see **Materials and equipment, 11.3**) to enhance heating conditions, resulting in a maintained polyol yield of 50% (**Table 4**, entry 2). Similar to the aminolysis with linear diamines, a mixture of different polymer types was hypothesized for the aromatic residue. This hypothesis was supported by the detection of seven tolyl groups between 1.7 and 2.2 ppm. Complete aminolysis products were identified for both configurational stereoisomers of TDI (**Figure 10a**) along with five different intermediates representing partially aminolysed isomers and fractions where the polyol remained bonded to both isocyanates of the isomer (**Figure 10b**).

Table 4. Aminolysis of PU Flexible Foam with 2,4-TDA – 2 grams scale[a]
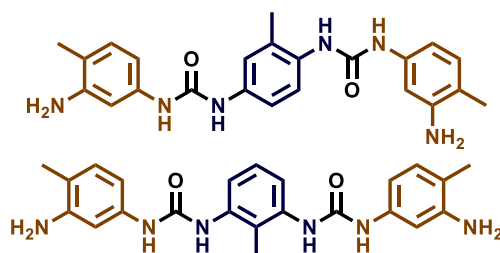

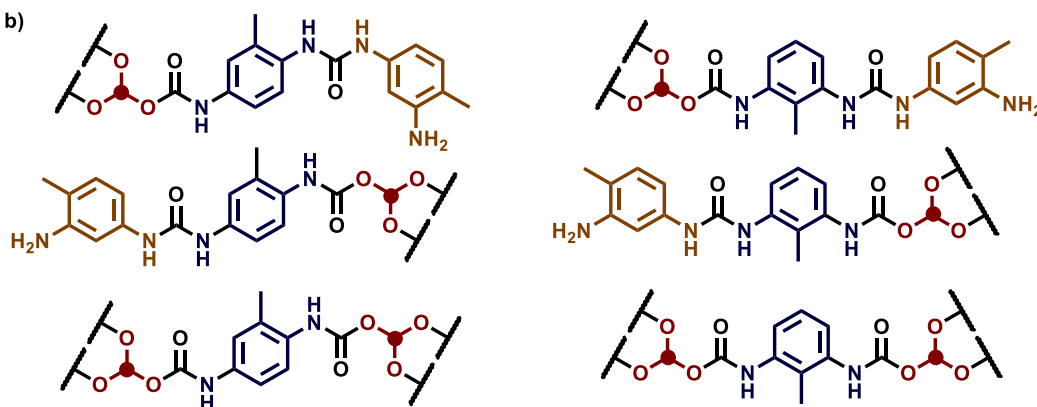| entry	DA	Polyol [mg]	Polyol [%][b]	Aromatic fraction [mg]	Change of reaction conditions
1	2,4-TDA	218	25	2280	-
2	2,4-TDA	681	50	1323	CO-tube

[a] Reactions performed as described in General Procedure 10.1.5. [b] Isolated yield. (DA diamine, TDA toluendiamine)

Figure 10: Desired products and intermediates of PU aminolysis with 2,4-TDA

a)

b)

For the PU shoe sole, the same reactions conditions were tested, but due to purification issues, any further improvements in the yield of polyol and aromatic fraction were put on hold. In the case of reaction with EDA **(Table 5, entry 1)**, it was not feasible to identify a repetitive structure for the aromatic

fraction. However, when HMDA was utilized (**Table 5,** entry 2), several structures were identified. Specifically, the aromatic fraction revealed the presence of four distinct intermediates, which corresponded to both complete (**Figure 11a)** and partial aminolysis (**Figure 11b)** of the initial urethane polymer. As previously mentioned, this particular polyurethane composition contains diisocyanate groups primarily composed of 4,4'-MDI, along with minor traces of 2,4'-MDI [10], consequently, the complete aminolysed fraction is a mixture of the two isomers.

The same behaviour was observed for the reaction with 4,4'-MDA as degradative agent (**Table 5**, entry 3). The substrates presented in the aromatic fraction could be correlated to the attended aminolysed product (**Figure 12a)** and from the same ^{1}H-NMR it was possible to detect two kind of intermediates, which based on MDI as the monomer, would represent the mono-aminolyzed and the di-aminolyzed adduct (**Figure 12b)** of flexible PU solids.

Table 5. Aminolysis of PU shoe sole – 250 milligrams scale[a]

Flexible rigid Polyurthane - shoe sole
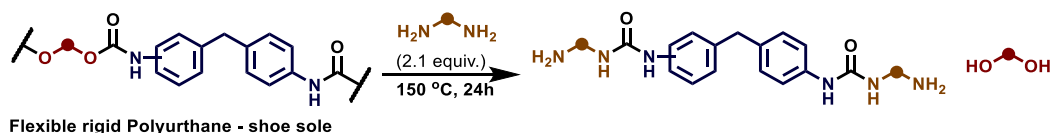
entry	DA	Polyol [mg]	Aromatic fraction [mg]	Change of reaction conditions
1	EDA	17	192	100° C [c]
2	HMDA[b]	595	1360	-
3	4,4-MDA	80	60	-

[a] Reactions performed as described in General Procedure 10.1.5 [b] performed with 2 grams of DA. [c] To avoid the boiling point of EDA (b.p. 116°C). (DA diamine, EDA ethylenediamine, HMDA hexamethyelendiamine, MDA methylenedianiline)

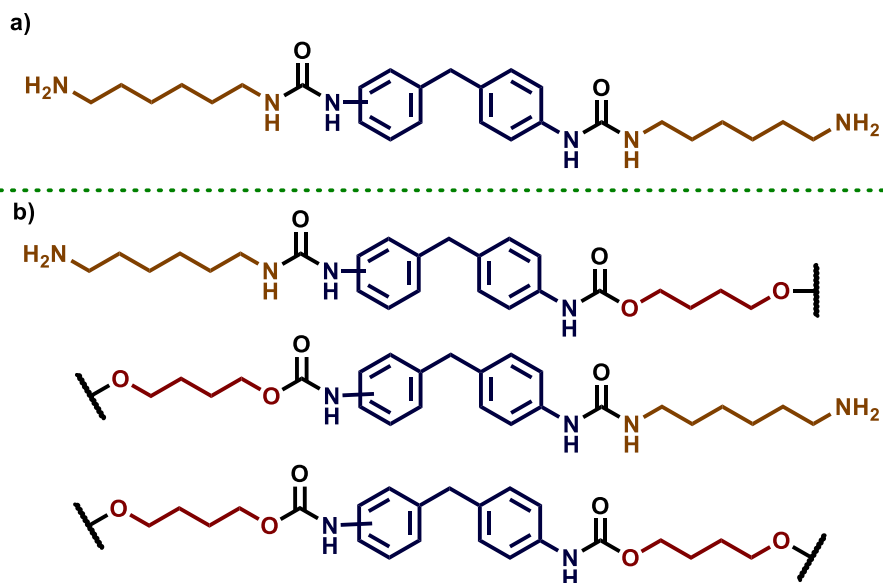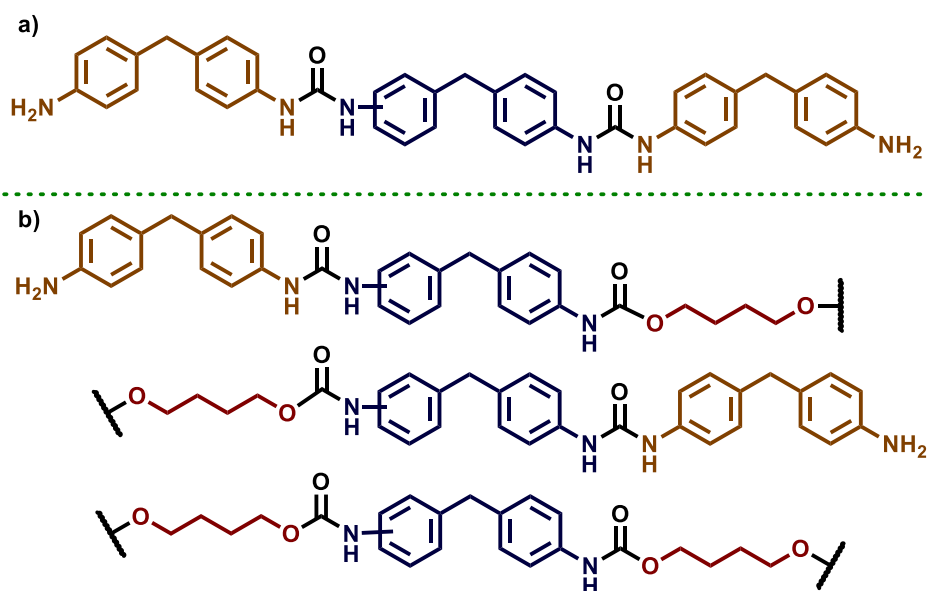**Figure 11:. Desired products and intermediates of PU shoe sole aminolysis with HMDA**

a)

b)

Figure 12: Desired products and intermediates of PU shoe sole aminolysis with 4,4'-MDA

a)

b)

For all reactions presented in this section the aminolysis process was not complete. As reported in literature, one possibility to further promote the formation of the desired polyols and aminolysis adduct is to increase the

temperature [38]. The rate of depolymerization is also related to the basicity of the chosen degrading agent, as more basic diamine result in higher yield of depolymerization [39]. Since the goal of this project was to evaluate the residual aromatic fraction, these reactions were tested just in the beginning of the project with the idea of a later evaluation of the reaction conditions.

7.2 SYNTHESIS OF MODEL SUBSTRATES:

In order to evaluate the deconstruction of the aromatic residues obtained from the aminolysis process, a range of model substrates were synthesised. Here, it was decided only to look at one isomer of the TDI to simplify the ensuing characterization. As such, three out of the four model substates acting as surrogate for the segments derived from the aminolysis of 2,4-TDI based PU, were obtained by reacting one equivalent of 2,4-TDI and two equivalents of DA. The chosen DA were EDA, HMDA and PT (para-toluidine) which gave as outcome the respectively formation of **Model 1**, **Model 2** and **Model 3** (see **Figure 13**). For **Model 4** (**Figure 13**), which served as a mimic for the hard segment obtained from aminolysis of 4,4'-MDI based PU materials, the reaction involved 1 equiv. of 4,4'-MDI and 2 equiv. of PT (See **General Procedure 7.1.1**). Here, a single isomer of MDI was selected to streamline further characterization. All the models were obtained in good yields (80 - 95%) and they were characterized by ^{1}H-NMR, ^{13}C-NMR and FT-IR (See **General Procedure 10.1.1**).

Figure 13: Synthesis of model substrates
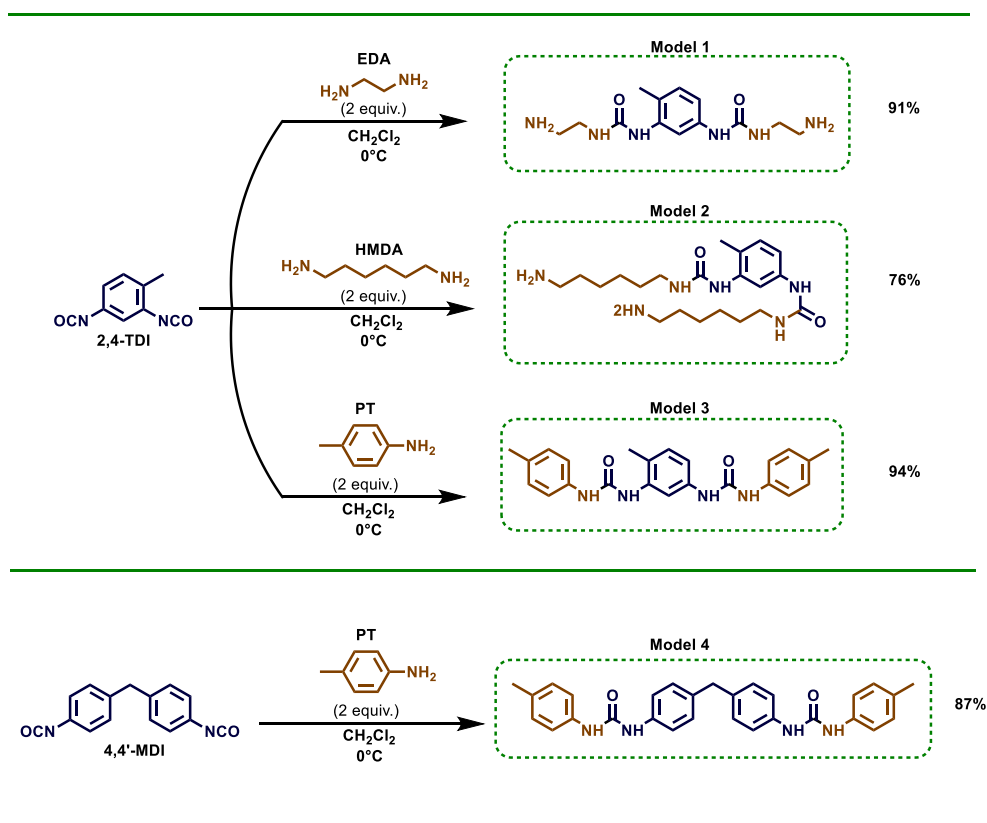
## 7.3 HYDROLYSIS OF MODEL SUBSTRATES:

As a way to valorise the hard segment obtained from the aminolysis of PU, hydrolysis was envisioned as a clean and ease way to break the urea-functionality. The initial hydrolysis reactions were performed on **Model 1**, one out of four of the different model substrates that were previously synthesized [34]. Both basic and acidic hydrolysis were then initially performed at 100°C. Working at relatively low temperature would from a safety perspective mean that reaction could be performed without specialized equipment so the reactions were performed in a 8 mL vial fitted with stirring bar and sealed with lid (See **General Procedure 10.1.2**). The reactions on Model 1 using 5 mL of 2M NaOH were performed at increasing reaction times of 3, 6 and 24 hours (**Table 6**, entries 1, 3 and 5) respectively, but just for the latter some traces of 2,4-TDA was detected. No conversion to the desired diamine was observed for hydrolysis performed in 5 mL of 2M HCl for 3 and 6 hours (**Table 6**, entries 2 and 4).

The temperature and the reaction time was then increased. While the initial experiments was performed in vials, these experiments were conducted in 45 mL autoclaves fitted with 30 mL poly(tetrafluoroethylene) inlay (See **General Procedure 10.1.2**, and **Materials and equipment 11.2**). During evaluation of acidic hydrolysis, the autoclave showed sign of deterioration, as such acidic conditions were abandoned for this procedure. In an autoclave set-up, the conversion of **Model 1** to 2,4-TDA in alkaline conditions reached 60% and 64% yield after 3 and 24 hours at 150 °C (**Table 6,** entries 6 and 7), respectively. On the contrary, increasing the reaction temperature to 200°C for 3 hours yielded 2,4-TDA in a quantitative yield (**Table 6,** entry 8). Similar outcomes were obtained for the hydrolysis of Model 2 that yielded 16% and 60% of 2,4-TDA after 3 and 24 hours under alkaline conditions (**Table 6**, entries 10 and 11), while alkaline hydrolysis at 200°C for 3 hours afforded 93% of 2,4-TDA (**Table 6**, entry 13).

Whit emphasis on the study reported by Medina-Ramos *et al.* (Described in **Theoretical background 6.2**) the hydrolysis at 150 °C in 5 mL of water was tested on 100 mg of both **Model 1** and **Model 2**. In each case the reaction

did not go to completion, as a partial recovery of diamine was obtained (**Table 6**, entries 9 and 14)**.**

Table 6: Hydrolysis of Model 1 and Model 2 [a]
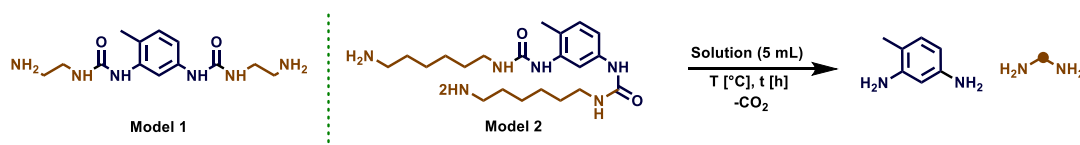
entry	Model	Solution	T [°C]	t [h]	2,4-TDA [%][b]
1	1	NaOH [2M]	100	3	nd
2	1	HCl [2M]	100	3	nd
3	1	NaOH [2M]	100	6	nd
4	1	HCl [2M]	100	6	nd
5	1	NaOH [2M]	100	24	traces
6	1	NaOH [2M]	150	3	60
7	1	NaOH [2M]	150	24	64
8	1	NaOH [2M]	200	3	100 [c]
9	1	H₂O	150	24	9
10	2	NaOH [2M]	100	24	traces
11	2	NaOH [2M]	150	24	60
12	2	NaOH [2M]	150	3	16
13	2	NaOH [2M]	200	24	93
14	2	H₂O	150	24	8

[a] Reactions performed as described in General Procedure 10.1.2. [b] Determined using ^{1}H NMR spectroscopy with 1,3,5 trimethoxybenzene as internal standard. [c] Isolated yield.

The same autoclave set-up was maintained for the alkaline hydrolysis of **Model 3**, resulting in 1% and 38% conversion to 2,4-TDA after 3 and 24 hours at 150 °C (**Table 7,** entries 1 and 2). Increasing the temperature at 200°C afforded an overall yield of 65% (**Table 7**, entry 3). At the same time **Model 4** was tested, the yield of conversion was calculated based on the quantity of 4,4'-MDA formed. For the reaction at 150°C for 24 hours only a mere 3% was obtained (**Table 8**, entry 1), while an increase in temperature

to 200°C yielded 26% of the desired 4,4'-MDA (**Table 8**, entry 2). Also for these models a test of hydrolysis with 5 mL of water at 150°C [24] was performed on the same moles of model, for **Model 3** it leaded a conversion of 8% in 2,4-TDA (**Table 7**, entry 4) while for **Model 4** the formation of 4,4'-MDA yielded a mere 3% (**Table 8**, entry 3). These results were not surprising considering the lower solubility of **Model 3** and **Model 4** as compared to **Model 1** and **Model 2**. The lower solubility was visually evident, as **Model 3** and **Model 4** could be filtered off from the solution after the hydrolysis.

Table 7: Hydrolysis of Model 3 [a]
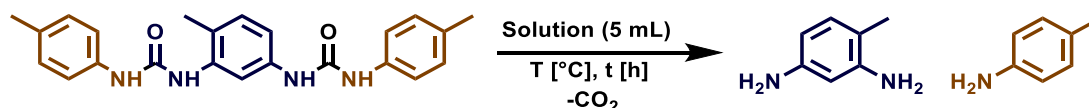
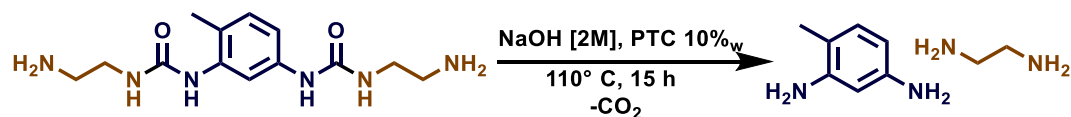| entry	Model	Solution	T [°C]	t [h]	2,4-TDA [%][b]
1	3	NaOH [2M]	150	3	1
2	3	NaOH [2M]	150	24	38
3	3	NaOH [2M]	200	24	65
4	3	H_2O	150	24	8

[a] Reactions performed as described in General Procedure 10.1.2. [b] Determined using ^{1}H NMR spectroscopy with 1,3,5 trimethoxybenzene as internal standard.

Table 8: hydrolysis of Model 4 [a]
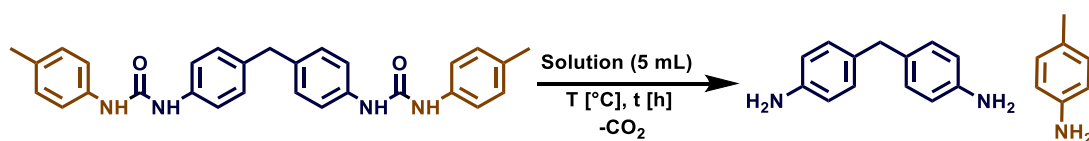
entry	Model	Solution	T [°C]	t [h]	4,4'-MDA [%][b]
1	4	NaOH [2M]	150	24	3
2	4	NaOH [2M]	200	24	26
3	4	H_2O	200	24	3

[a] Reactions performed as described in General Procedure 10.1.2. [b] Determined using ^{1}H NMR spectroscopy with 1,3,5 trimethoxybenzene as internal standard.

7.4 HYDROLYSIS WITH PHASE TRANSFER CATALYST:

Since the main problem of these substrates was the solubility, a range of phase transfer catalysts (PTC) were tested in order to increase the interaction between nucleophile and the substrate. In this case the phase transfer has worked in a solid-liquid system where the substrate is poorly soluble [40]. Ideally the added catalyst should aid the solubilization of the solid reactant in the liquid phase, enabling in this way better contact between the two reactive species. Additionally, in most of the cases it is necessary to work with milder conditions due to the low thermal stability [41].

Initially, a screening of different phase transfers was done on **Model 1**, the chosen salts were tested with the same reaction conditions. Tetraoctylammonium bromide (TOAB) and trihexyl(tetradodecyl) phosphonium bromide (THTDPB) provided a yield lower than 10% (**Table 9,** entries 4 and 6) while a better conversion in aniline was obtained for tetrabutylammonium chloride (TBAC), tetrabutylammonium bromide (TBAB) and tetrabutylammonium hydrogensulfate (TBAS) (**Table 9,** entries 1, 2, 3). Only dodecyltrimethylammonium chloride (DTMAC) yielded 32% in 2,4-TDA that was the higher obtained. The latter one was then chosen for a more deep study.

Table 9: Hydrolysis of Model 1 using phase transfer catalyst (PTC) [a]

entry	PTC	2,4-TDA [%][b]
1	TBAC	14
2	TBAB	19
3	TBAS	24
4	TOAB	10
5	DTMAC	32
6	THTDPB	6

| 7 | none | 1 |

DTMAC yielded the highest conversion for **Model 1** in TDA (entry 5). To achieve a quantitative yield, adjustments were made to the reaction conditions. The introduction of an organic phase, toluene, led to a 55% yield in TDA at 110°C (**Table 10**, entry 1). This identical reaction setup was subsequently applied to **Model 2**, resulting in a 28% conversion to 2,4-TDA (**Table 10**, entry 2).
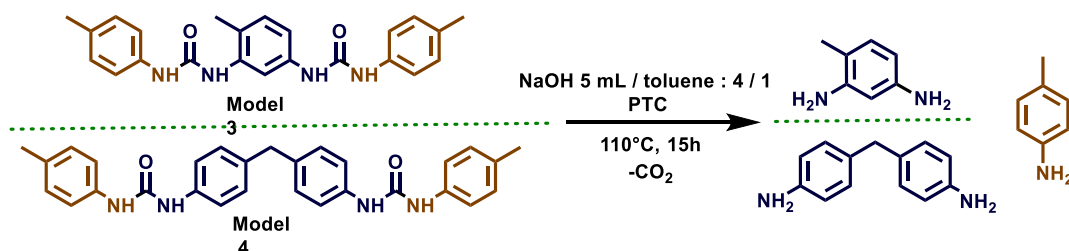
Table 10: Hydrolysis of Model 1 and Model 2 using a phase transfer catalyst [a]
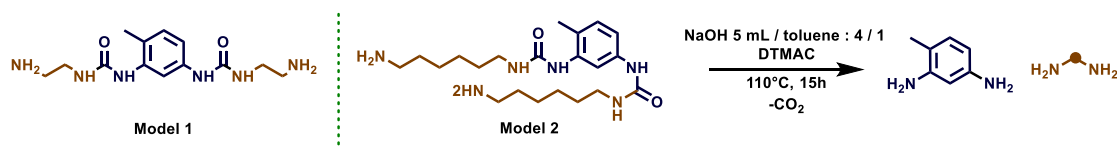
entry	model	PTC	2,4-TDA [%][b]
1	1	DTMAC	55
2	2	DTMAC	28

Table 11: Hydrolysis of Model 3 and Model 4 with phase transfer catalyst [a]

entry	Model	PTC	2,4-TDA [%][b]
1	3	DTMAC	16
3	4	DTMAC	1

[a] Reactions performed as described in General Procedure 10.1.4. [b] Determined using ^{1}H NMR spectroscopy with 1,3,5 trimethoxybenzene as internal standard.

For **Model 3** and **Model 4** was decided to test the reaction at higher temperature so a more temperature resistant phase transfer was chosen. From the literature, tetrabutylammonium hydrogensulfate was proven to be stable at temperature of 260°C, [41] as such it was tested under the same reaction conditions up to 150°C.

Here, a 16% yield of 2,4-TDA for **Model 3** was obtained (**Table 11,** entry 1), while traces of 4,4'-MDA were obtained for **Model 4** (**Table 11,** entry 2). These yields were similar to the ones obtained without phase transfer so the solubility of the substrate is not increased even if a phase transfer catalyst is utilized.

7.5 HYDROGENATION:

The model substrates were subjected to catalytic hydrogenation using either ruthenium, manganese or iridium catalyst to evaluate their capacity for generating dianilines from the hard segment obtained via aminolysis. In the case of **Model 1,** our initial trials employed the commercial Ir-^{iPr}MACHO catalyst using the conditions outlined in literature based on **Theoretical background 6.3** [32]. However, these attempts only yielded a low conversion of **Model 1**, affording a mere 18% of 2,4-TDA (**Table 12,** entry 1). This could be due to solubility issues, as such, considering that the substrate is fully soluble in DMSO, the reaction was repeated under otherwise similar conditions using DMSO as solvent but the yield in 2,4-TDA was 8% (entry 2). Consequently, the reaction duration was prolonged, yet the yield remained unchanged (entry 3). In an effort to enhance the performance of the Ir catalyst, the reaction temperature was increased to 180 °C, which provided a quantitative yield of 2,4-TDA (entry 4).

Concurrently, we explored the application of a Ru-^{iPr}PNN known for its ability to decompose amide substrates in DMSO as stated in **Theoretical background 6.3** [15]. However, the reaction was far from completion at both the 24-hour (entry 5) and 48-hour (entry 6) marks with a yield of 5% and 8% respectively. In this case the increase of temperature was avoided since the combination of pressure and heating could lead to the decomposition of the solvent with a possible explosion [42].

Knowing the possible esterification of the substrate and in an effort to find a more environmentally friendly solvent [43], we evaluated isopropanol for the Ir-^{iPr}MACHO catalyzed hydrogenation of urea [34] [35]. In this experiment, all conditions remained the same except for the temperature, which was set at 180° C based on its efficiency in the previous reactions, resulting in a 63% yield of 2,4-TDA (entry 7). Maintaining same temperature and solvent, Ru-^{iPr}MACHO and Mn-^{iPr}MACHO catalysts were also tested and much to our delight the hydrogenation provided a 72% (entry 8) and 52% yield of 2,4-TDA (entry 9), respectively.
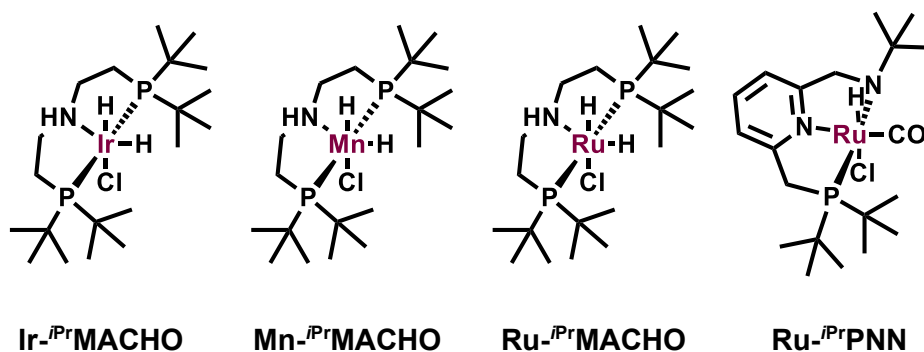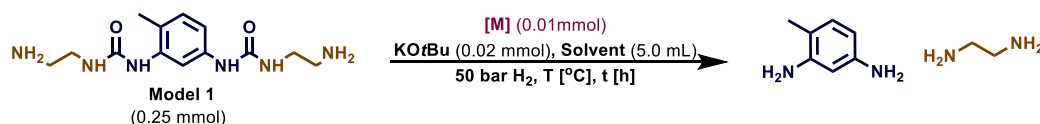
Ir-^{iPr}MACHO   Mn-^{iPr}MACHO   Ru-^{iPr}MACHO   Ru-^{iPr}PNN

Table 12. Catalytic Hydrogenation of Model 1 [a]

entry	catalyst	solvent	T [ºC]	t [h]	2,4-TDA (%)[b]
1	Ir-^{iPr}MACHO	THF	150	24	18
2	Ir-^{iPr}MACHO	DMSO	150	24	8
3	Ir-^{iPr}MACHO	DMSO	150	48	8
4	Ir-^{iPr}MACHO	THF	180	24	quant.
5	Ru-^{iPr}PNN	DMSO	150	24	5
6	Ru-^{iPr}PNN	DMSO	150	48	8
7	Ir-^{iPr}MACHO	iPrOH	180	24	63
8	Ru-^{iPr}MACHO	THF	180	24	72
9	Mn-^{iPr}MACHO	THF	180	24	52

[a] Reactions performed as described in General Procedure 10.1.3. [b] Determined using ^{1}H NMR spectroscopy with 1,3,5 trimethoxybenzene as internal standard.

Moving on from **Model 1**, the same trend was observed for the catalytic hydrogenation of **Model 2.** Here, using Ir-^{iPr}MACHO under typical literature conditions afforded no 2,4-TDA formation (**Table 13,** entry 1) and starting material could be reisolated. Despite attempts to improve the yield working with DMSO the yield never exceeded 23% (entry 2). With the Ru-^{iPr}PNN complex in DMSO the yield of 2,4-TDA was around 10% (entry 3), even

when the reaction time was extended from one day to two days (entry 4) the yield reached a mere 6%. Only when the temperature was set to 180°C we achieved better yield of TDA using Ir catalyst that reached 90% for the reaction in 24 hours (entry 5) and quantitative yield after 48 hours (entry 6). Moreover, using *i*PrOH yielded 70% of 2,4-TDA (entry 7).

**Table 13. Catalytic Hydrogenation of Model 2 [a]**

entry	catalyst	solvent	T [ºC]	t [h]	2,4-TDA (%)[b]
1	Ir-*iPr*MACHO	THF	150	24	nd
2	Ir-*iPr*MACHO	DMSO	150	24	23
3	Ru-*iPr*PNN	DMSO	150	24	12
4	Ru-*iPr*PNN	DMSO	150	48	6
5	Ir-*iPr*MACHO	THF	180	24	90
6	Ir-*iPr*MACHO	THF	180	48	quant.
7	Ir-*iPr*MACHO	*i*PrOH	180	24	70

[a] Reactions performed as described in General Procedure 10.1.3. [b] Determined using ^{1}H NMR spectroscopy with 1,3,5 trimethoxybenzene as internal standard.

Reactions carried out on **Model 3** exhibited improved yields even at 150°C. The utilization of Ir-*iPr*MACHO catalyst in THF at 150°C resulted in 87% yield (**Table 14,** entry 1) while transitioning from THF to DMSO as the solvent provided a similar reaction yield of 72% (entry 2). Simultaneously, utilizing a Ru-*iPr*PNN catalyst in DMSO produced a 66% yield of 2,4-TDA (entry 3), which remained unchanged even when the reaction was extended for two days (entry 4). Since the Ru catalyst demonstrated efficacy for this particular model, a shift to THF was considered to streamline subsequent steps, this led to a yield of 77% (entry 5). Similar to the previous hydrogenation processes, raising the temperature for the Ir catalyst to 180°C yielded a

quantitative 2,4-TDA yield (entry 6). Additionally, a trial utilizing isopropanol was conducted, with an outcome of 95% of 2,4-TDA after 24 hours at 150°C (entry 7).

Table 14. Catalytic Hydrogenation of Model 3 [a]
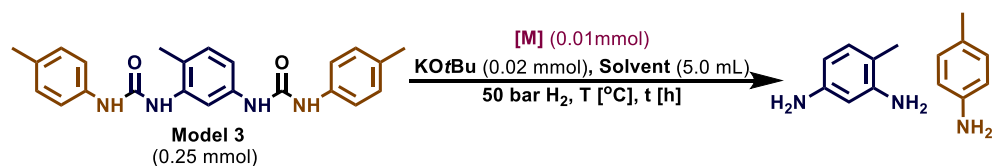
entry	catalyst	solvent	T [°C]	t [h]	2,4-TDA (%)[b]
1	Ir-^{iPr}MACHO	THF	150	24	87
2	Ir-^{iPr}MACHO	DMSO	150	24	72
3	Ir-^{iPr}MACHO	DMSO	150	24	66
4	Ru-^{iPr}PNN	DMSO	150	48	66
5	Ru-^{iPr}PNN	THF	150	48	77
6	Ir-^{iPr}MACHO	THF	180	65	quant.
7	Ir-^{iPr}MACHO	iPrOH	150	24	95

[a] Reactions performed as described in General Procedure 10.1.3. [b] Determined using ^{1}H NMR spectroscopy with 1,3,5 trimethoxybenzene as internal standard.

Given the comparable electronic density of **Model 3** and **Model 4**, the best conditions were conducted for the latter. In the presence of an Ir catalyst in THF, a mere 2% of 4,4'-MDA was detected at 150°C (**Table 15,** entry 1). However, elevating the temperature to 180°C led to a significant improvement, with the yield in 4,4'-MDA increasing to 40% with no other changes in the parameters (entry 2) . On the other hand, using a Ru-^{iPr}PNN catalyst in DMSO resulted in 86% yield at 150°C (entry 3). Gratifyingly, changing the solvent to iPrOH resulted in 90% of conversion to 4,4'-MDA. (entry 4).

Table 15. Catalytic Hydrogenation of Model 4 [a]
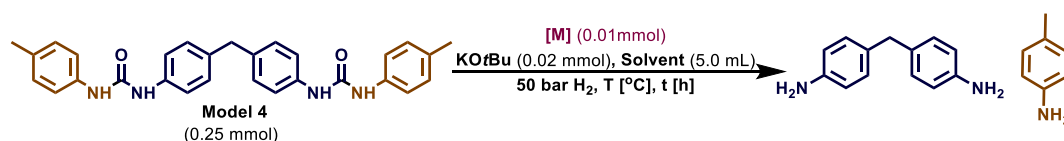
entry	catalyst	solvent	T [°C]	t [h]	4,4'-MDA (%)[b]
1	Ir-^{iPr}MACHO	THF	150	24	2
2	Ir-^{iPr}MACHO	THF	180	24	40
3	Ru-^{iPr}PNN	DMSO	150	24	86
4	Ir-^{iPr}MACHO	iPrOH	180	24	90

[a] Reactions performed as described in General Procedure 10.1.3. [b] Determined using ^{1}H NMR spectroscopy with 1,3,5 trimethoxybenzene as internal standard.

7.5.1 RU-^{iPr}PNN catalyst comparison between the different models

The Ru-^{iPr}PNN catalyst was synthesized following the general procedure [44] (see **General procedure 10.1.6**). The Ru-^{iPr}PNN catalyst was chosen as it performed well in DMSO, being the only solvent that solubilize the substrates completely. However, a mere conversion of 5% and 12% in 2,4-TDA at 150° degrees was obtained for **Model 1** and **Model 2** respectively, while for **Model 3** and **Model 4** the yields reached 66% and 76% underlining a clear increase. It was possible to underline how the substrates that present an aromatic functional group bonded to the nitrogen atom gave a better hydrogenation. Looking at the hypothesised intermediates it was acceptable to presume that phenyl groups compensate for the loss of stability caused by the weakened interaction between the amide nitrogen atoms and the carbonyl groups [33].

Moreover, it is important to note that the mechanism described in the **Theoretical background 6.3** pertains to a single urea bond, however, each molecule completely hydrogenate in these reactions presented two ureic bonds. It became apparent that an additional cycle of the Ru catalyst was required for each urea derivative due to the dual cleavage of the C-N bond, leading to a faster decreasing in activity of the catalyst.

7.5.2 Influence of the metal centre

As stated in the introduction the role of the metal centre during the hydrogenation reactions is central and it is possible to study its effect by maintaining the same ligand while changing the nature of the metal. The selection of the MACHO ligand for this study was predicated upon previously demonstrated efficacy in catalysing hydrogenation of urea residues. During the reactions on **Model 1** the yield of 2,4-TDA had a decreasing trend when the metal of the MACHO catalyst was changed from Ir > Ru > Mn. Thus trend was also evident for polyurethane hydrogenation, [33] stated in the introduction. (**Theoretical background 6.3**).

Figure 14: Yield of 2,4-TDA after hydrogenation of Model 1
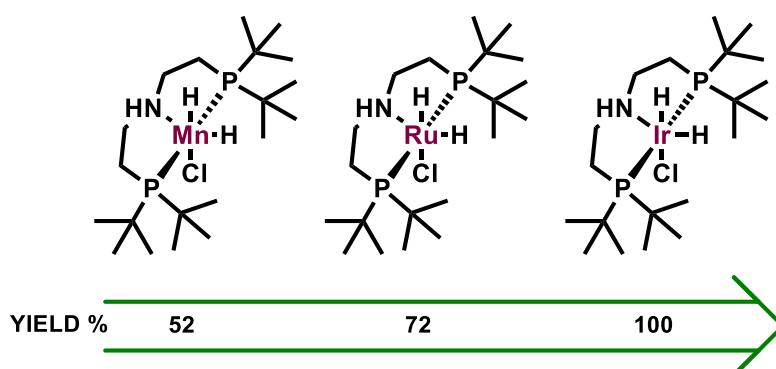
Considering that in our case the reaction temperature was 180° C it is acceptable to consider that the dissociation energies of ^{iPr}MACHO ligand from Mn and Ru centre (34.1 and 44.7 kcal/mol respectively) [33] were reached before the reaction was complete leading in this way a lower yield in 2,4-TDA.

7.5.3 Influence of isopropanol as solvent

As summarize in **Table 16** the reactions conducted with Ir-^{iPr}MACHO catalyst in isopropanol gave good to high yields for all the models but the reaction was more efficient when the models presented an aromatic group in the amide of the urea bond. Even though it has been noted that isopropanol acts as both a solvent and a hydrogen donor in the hydrogenation reaction, we

maintained a hydrogen pressure of 50 bar to ensure comparability across reactions.

Table 16: *Comparison of different model substrates when the solvent is changed. Same reaction conditions for all the entries.*
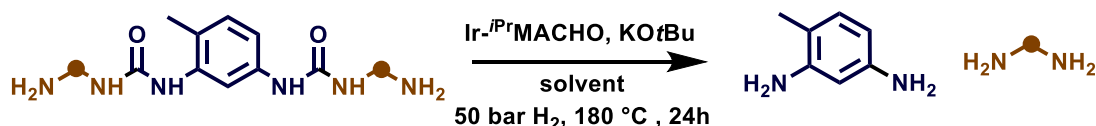
entry	model	2,4-TDA [%] in THF	2,4-TDA [%] [a] in *i*PrOH
1	1	quant.	63
2	2	quant.	70
3	3	87	quant.
4	4	40	90 [b]

[a] Determined using ^{1}H NMR spectroscopy with 1,3,5 trimethoxybenzene as internal standard. [b] Yield in 4,4'-MDA.

As elucidated by Werner and Liu, the reaction in isopropanol follows a two-step mechanism, initially the carbamate is formed and successively it undergoes hydrogenation into amine and methanol. The establishment of carbamate formation was substantiated through continuous monitoring, showcasing the evolving formation and decomposition of carbamate over time [34]. The same behaviour was expected for these reactions and in the case of **Model 1**, analysis of the spectra revealed the presence of six peaks ranging from 8.0 to 8.7 ppm, which can be attributed to N-H peaks arising from urea or carbamate bonds. Furthermore, the distinctive doublet resulting from the coupling of isopropyl carbamate was identified between 1.0 and 1.2 ppm, effectively confirming carbamate formation. Similar patterns were observed for **Model 2**, where eight peaks spanning from 7.9 to 9.3 ppm were detected, signifying the persistent presence of intermediates featuring ureic and carbamate bonds. These findings were further supported by a series of doublets within the range of 1.1 to 1.2 ppm, confirming the presence of carbamate bonds.

The reactions conducted on the aromatic substrates yielded significantly improved outcomes (**Table 16,** entry 3 and 4). Notably, no peaks were detected in the region spanning from 8.0 to 9.0 ppm, indicating a comprehensive decomposition of the ureic models and of any residual carbamate.

In this case the using of isopropanol induced a better reaction yield for substrates that presented an aromatic group. Since the hypothesis was the formation of a carbamate intermediate that was the same for every reaction regardless the nature of the urea residue **Scheme 12, 1a** (different structure for 4,4'-MDI based model) it was possible to assume that in path 2 the intermediate **2a** had a different reactivity depending on the functional group bonded to the amine.

Scheme 12: Proposed mechanism for hydrogenation with *i*PrOH as solvent
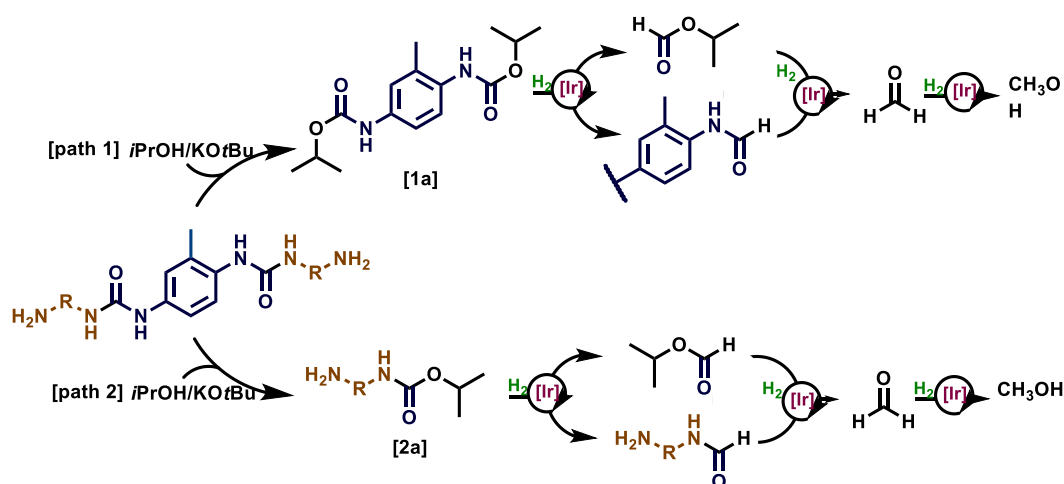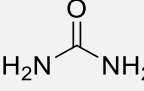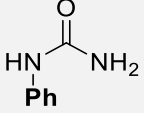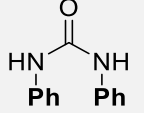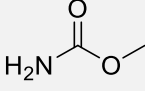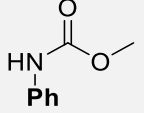
Figure 15: Intermediates of path 2 considering esterification of Model 1 and Model 3

2a intermediates:

48
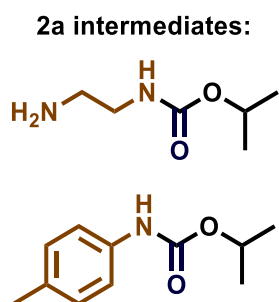
During a theoretical study conducted by Rong and coworkers [33] it was demonstrated that the incorporation of a phenyl group on the amine atom decreased the energy barriers of hydride transfer, leading to an increase of activity of the hydrogenation process. Adding phenyl groups to the amide nitrogen atoms reduces the energy barriers for hydride transfer **Table 17**. This is probably because the phenyl groups compensate for the loss of stability caused by the weakened interaction between the amide nitrogen atoms and the carbonyl groups [33].

Table 17: Trend of HOMO-LUMO gap and free energy when a Ph group is added. The considered reaction is hydrogenation of C=O using Ir-^{iPr}MACHO catalyst. Adapted from [33]

	H_2N—C(=O)—NH_2	$HN(Ph)$—C(=O)—NH_2	$HN(Ph)$—C(=O)—$NH(Ph)$	H_2N—C(=O)—O—	$HN(Ph)$—C(=O)—O—
HOMO-LUMO gap [eV]	0.46	0.35	0.34	0.48	0.35
$\Delta G^{\neq}$	44.6	32.8	27.9	38.1	31.1

This might explain the better reactivity of the aromatic models in presence of Ir-^{iPr}MACHO catalyst with isopropanol as solvent.

8 FUTURE WORK

Parallely to this study an interesting paper was published regarding the aminolysis process in which several optimization for this process might be applied to obtain a complete degradation of the starting PU into the desired polyol and the aromatic fraction. Some useful improvements might be the use of polyol as solvent for the reaction [45] or the addition of a Lewis acid catalyst such as TBD:MSA [37].

Moreover, to completely optimize the hydrogenation reactions conducted in *i*PrOH, some investigation of the mechanism should be performed, starting from control reactions without the addition of the catalyst, in this way it should be possible to understand if the carbamate intermediate is formed and if its formation facilitate the hydrogenation process.

In the end, the optimized reactions should also be tested on real aromatic fraction to effectively close the molecular recycling of the PU samples.

9 CONCLUSION

In conclusion, this study addresses the critical challenge of PU recycling in the face of a rapidly expanding global market. The comprehensive molecular recycle of PU, particularly emphasizing the evaluation of the aromatic fraction post-polyol filtration, was demonstrated being possible through aminolysis. During this project we investigated the decomposition through hydrolysis and hydrogenation of the four different models that were synthesized in order to investigate the general motif of the aromatic fraction obtained from aminolysis of PU.

For each model, we successfully obtained several valid possibilities which could be considered for the decomposition of the aromatic fraction. Specifically, for **Model 1** and **Model 2**, which presents a motif similar to the residue of aminolysis of EoL PU from mattress with linear diamines (EDA and HMDA), the hydrolysis reaction provided complete conversion to 2,4-TDA at 200°C under alkaline conditions. Moreover, the hydrogenation reactions of these models gave good yield, in particular the utilization of Ir-^{iPr}MACHO at 180°C furnished complete decomposition.

Lastly, for **Model 3** and **Model 4** which imitate the residues of aminolysis with aromatic diamines (2,4-TDA and 4,4'-MDA), the hydrogenation reactions foresee better results with both Ir-^{iPr}MACHO and Ru-^{iPr}PNN catalysts, especially with the utilization of *i*PrOH as solvent, while hydrolysis reactions might necessitate more drastic conditions to reach conclusion.

10 EXPERIMENTAL PART:

10.1 GENERAL PROCEDURES:

10.1.1 Synthesis of model substrates:
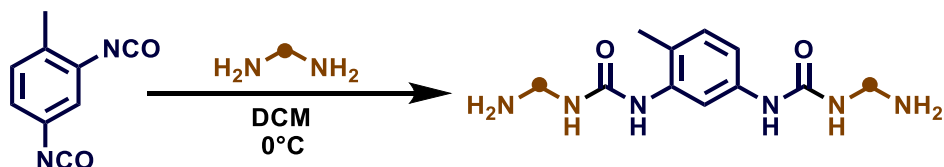
Scheme 13: General coupling reaction for model substrates with TDI as diisocyanate

For **Model 1**, **Model 2** and **Model 3** 2,4-TDA (2.00 g, 11.5 mmol) was placed in a dry 50 mL round bottom flask with a fitted magnet. The flask was sealed with a septum and a balloon of N_2 was added. Anhydrous DCM (10 mL) was added with a syringe in order to dissolve the diisocyanate. The diamine (2.0 eq, 23.0 mmol) was also placed in a dry 50 mL round bottom flask with a magnet, sealed with septum and dissolved with anhydrous DCM (20 mL) under a N_2 atmosphere and cooled to 0 °C. The diisocyanate solution was added using a syringe to the solution of diamine resulting in the formation of a white precipitate. The reaction was stirred for 24 h allowing the temperature to rise. The next day the precipitate was filtered, washed with DCM (3 x 10 mL) and dried under reduced pressure to obtain product.

Table 19: Moles of reagents used for the synthesis of model substrates

entry	DA	n diamine [mmol]	n diisocyanate [mmol]	Yield (%)[a]	Model
1	EDA	22.9	11.5	91	1
2	HMDA	22.9	11.5	76	2
3	PT	18.1	8.6	94	3

[a] Isolated yield.

The synthesis of **Model 4** was based on the above procedure were 4,4'-MDI (8.0 mmol) was used instead of 2,4-TDA and p-toluidine was used as the amine (16.8 mmol).

52
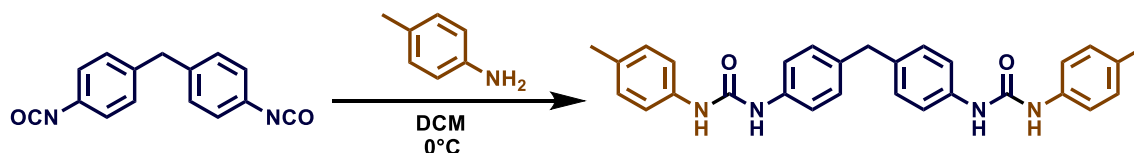
Scheme 14: General coupling reaction for model substrates with MDI as diisocyanate

10.1.2 Hydrolysis of model substrates:

In a PTFE inlay with fitted stirring bar were added 100 mg of model substrate and NaOH 2M aqueous solution (5 mL). The inlay was placed in an autoclave and sealed using a hex key. The autoclave was then placed in a pre-heated (150 °C – 200 °C depending on the reaction) aluminium block and stirred at 1000 rpm for 3 or 24 hours. After that, the autoclave was carefully opened and the probe was washed with small amount of DCM. The aqueous phase was filtered through a small cotton plug and extracted with DCM (3 x 15 mL). The combined organic phases were washed with brine, dried over MgSO$_4$ and filtered before solvent was removed under reduced pressure.

10.1.3 Hydrogenation of model substrates:

Working in an argon filled glovebox, catalyst (0.01 mmol), KO*t*Bu (0.02 mmol) and model substrates (0.25 mmol) were added to a PTFE inlay. Solvent (5 mL) was added and the inlay was placed in an autoclave that was carefully sealed using a hex key. The latter was taken out of the glovebox, connected to a 5000 Multi Reactor System, pressurize with 50 bar of H$_2$ (99.999% purity) from Air Liquid and finally placed in a pre-heated aluminium block specially designed to fit the vessels. The reaction was left stirring at a predefined temperature for the extend of the reaction, after which the autoclave was left to cool to room temperature. Here, the autoclave was depressurise under control settings using the 5000 Multi Reactor System and carefully opened using a hex key. The reaction mixtures was filtered through a cotton plug into a 50 mL round bottom flask and the solvent was removed

under reduced pressure. 1,3,5-trimethoxybenzene was added as internal standard for NMR.

10.1.4 Hydrolysis with phase transfer catalyst:

The screening of phase transfer catalysts on **Model 1** was performed in 8 mL vials fitted with a stirring bar. Here, **Model 1** (50 mg, 0.17 mmol) was along with catalyst (10 wt%) and 4 mL of NaOH 32% added to the vial. The reactions were run for 15 hours at 110°C. After the reaction, the water phase was extracted with DCM (3 x 15 mL), the combined organic phase was dried over $MgSO_4$, filtered and concentrated under reduced pressure, before the sample was analysed using 1,3,5-trimethoxybenzene as an internal standard for NMR.

10.1.5 Aminolysis of PU:

In a 8 mL vial fitted with stirring bar foam (250 mg) and diamine (2.1 eq) were added. The equivalents were calculated considering the number of urethane bonds present in the starting polyurethanes**.** The tested substrate were analysed in the article. [10] The vial was sealed with a septum and equipped with a N_2 balloon before being placed in a pre-heated aluminium block. The reaction was left stirring for 24 h.

The reactions on 2 grams of sample were based on the above procedure and initially performed in a 50 mL round bottom flask and only later set up in a CO-tube as reactor for improving the heating.

The polyol was extracted from the mixture with cyclohexane that was directly added to the vial / flask and left stirring for several hours. A porous funnel was used for the separation of the residue and the solvent. These steps of extraction and separation were repeated at least 4 times. All the extractions were recovered in a pre-weigh round bottom flask where the solvent was then evaporated under reduced pressure. The aromatic residue was left dry overnight and the next day stored in vial while the polyol was weight and stored in a vial after being dissolved in DCM.

For some polyol samples acidic extraction with HCl 1M was necessary to remove residual diamines.

10.1.6 Synthesis of Ru^{iPr}PNN catalyst:
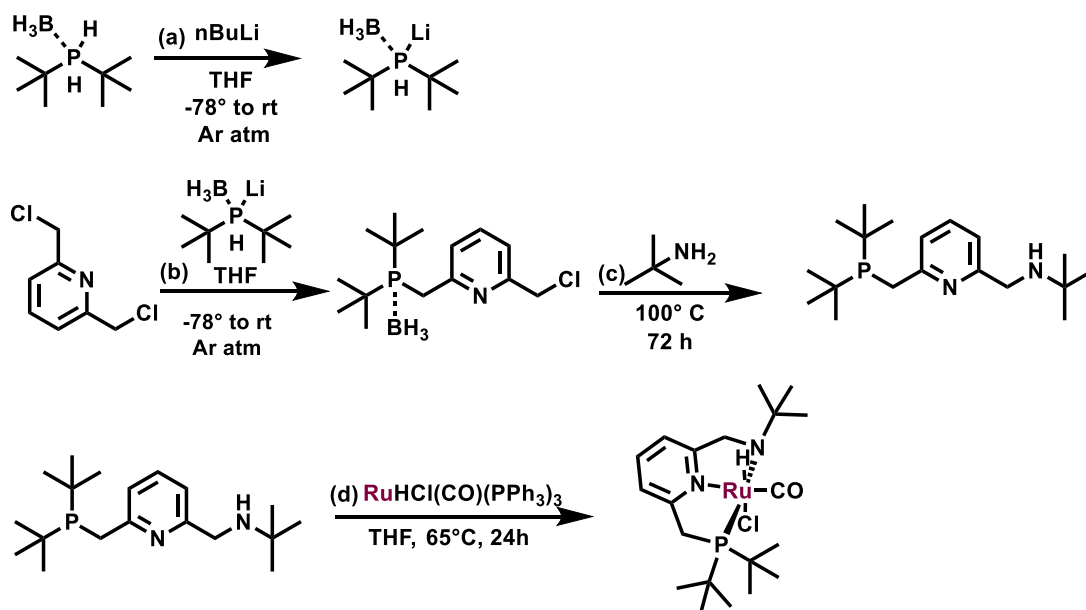
Scheme 15: Reactions for the synthesis of Ru^{iPr}PNN catalyst

Synthesis of ^{iPr}PNN ligand was conducted following a previously published method. [46] Involving sequential phosphorylation and amination of 2,6-bis(chloromethyl)pyridine with di-tert-butylphosphine borane and tertbutyl amine respectively.

In an ice bath, to a dry 3-neck round bottom flask fitted with a stirring bar and septas was under an atmosphere of argon added borane di(tert-butyl)phosphine (1.14 g, 7.08 mmol) and consequently 40 mL of anhydrous THF (40 mL). Next, *n*BuLi (in hexane, 5.0 mL, 1.4 M, 7.14 mmol) was added and was left to stir **(Scheme 15, a)**.

Subsequently, a solution of 2,6-bis(chloromethyl)pyridine (1.00 g) anhydrous THF (30 mL) was prepared and added dropwise to the solution containing the deprotonated phosphine. The reaction was left reacting for 24 hours allowing the temperature to rise **(Scheme 15, b)**. The product was isolated by column chromatography using as eluent ethyl acetate : hexane (1:10) with

a gradual increase of ethyl acetate. This afforded product as a white solid (0.49 g , 1.6 mmol) in a 29% yield.

Next, monophosphine-6-(chloromethyl)pyridine (0.49 g , 1.6 mmol) was transferred in a CO-tube, sealed with PTFE/silicon seals, where an excess of tertbutylamine was added (4 mL), it was used as solvent as reported in literature. The Co-tube was carefully sealed and the system was heated at 100°C at 800 rpm of stirring for 24 hours **(Scheme 15, c)**. After checking the conversion with H-NMR and P-NMR, more tertbutyl amine was added and the reaction was left stirring and heating for 48 hours. Then, excess of tertbutylamine was removed under reduced pressure. The resulting residue was dissolved in pentane and filtered through celite to remove any salts. This afforded the corresponding BH_3-deprotected phosphine and amine substituted ligand as viscous pale yellow oils with 62% yield.

Ru(H)(Cl)(CO)(PPh$_3$)$_3$ (443.0 mg, 0.46 mmol) was placed in a Co-tube fitted with stirring bar and dissolve in THF (5 mL), the previous synthesized ligand ^{iPr}PNN (150.4 mg , 0.46 mmol) was added and the reaction was stirred at 65°C overnight **(Scheme 15, d)**. The system was cooled down to room temperature and the solvent was concentrated to one third of its volume. Pentane was then added to precipitate the product which was filtered and washed with ether to afford Ru-^{iPr}PNN as pale yellow solid (165 mg) in a 72% yield.

10.2 CHARACTERIZATION:

Model 1: 1,1'-(4-methyl-1,3-phenylene)bis(3-(2-aminoethyl)urea):
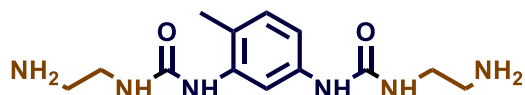
^{1}H NMR (400 MHz, DMSO) δ 8.43 (s, 1H), 7.72 (s, 1H), 7.62 (s, 1H), 7.14 (m, 1H), 6.93 (d, *J* = 8.4 Hz, 1H), 6.64 (s, 1H), 6.10 (d, *J* = 6.0 Hz, 1H), 3.38 (s, 4H), 3.16 (s, 3H), 3.13 – 3.02 (m, 1H), 2.69 – 2.57 (m, 1H), 2.08 (s, 3H).

^{13}C NMR (101 MHz, DMSO) δ 155.9, 155.9, 138.9, 138.6, 130.4, 119.9, 112.2, 110.8, 41.9, 17.7.

Model 2: 1,1'-(4-methyl-1,3-phenylene)bis(3-(6-aminohexyl)urea):
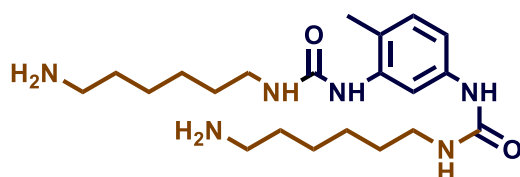
^{1}H NMR (400 MHz, DMSO) δ 8.26 (s, 1H), 7.71 (s, 1H), 7.48 (s, 1H), 7.17 – 7.05 (m, 1H), 6.91 (d, *J* = 8.6 Hz, 1H), 6.51 (s, 1H), 5.96 (s, 1H), 3.06 (s, 4H), 2.07 (s, 3H), 1.36 (m, 12H).

^{13}C NMR (101 MHz, DMSO) δ 155.7, 139.1, 138.7, 130.3, 119.4, 111.9, 110.4, 30.3, 26.6, 17.7.

Model 3: 1,1'-(4-methyl-1,3-phenylene)bis(3-(p-tolyl)urea:
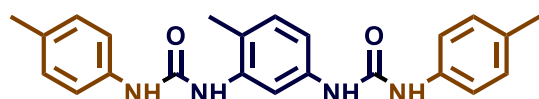
^{1}H NMR (400 MHz, DMSO) δ 8.93 (s, 1H), 8.57 (s, 1H), 8.39 (s, 1H), 7.92 (d, *J* = 2.2 Hz, 1H), 7.82 (s, 1H), 7.34 (dd, *J* = 12.6, 8.4 Hz, 3H), 7.18 (dd, *J* = 8.2, 2.3 Hz, 1H), 7.12 – 7.01 (m, 4H), 2.24 (s, 4H), 2.24 (s, 4H), 2.17 (s, 3H).

^{13}C NMR (101 MHz, DMSO) δ 153.0, 152.9, 138.4, 138.1, 137.8, 137.7, 130.9, 130.9, 130.7, 129.7, 129.6, 120.7, 118.6, 118.5, 118.5, 112.8, 111.0, 20.8, 17.7.

Model 4: 1,1'-(methylenebis(4,1-phenylene))bis(3-(p-tolyl)urea):
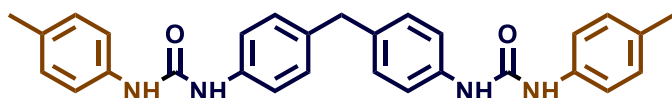
^{1}H NMR (400 MHz, DMSO) δ 8.50 (d, *J* = 13.9 Hz, 4H), 7.33 (dd, *J* = 10.8, 8.5 Hz, 8H), 7.09 (dd, *J* = 15.4, 8.6 Hz, 8H), 3.80 (s, 2H), 2.23 (s, 6H).

^{13}C NMR (101 MHz, DMSO) δ 153.1, 138.1, 137.6, 135.4, 130.9, 129.6, 129.4, 118.8, 118.7, 118.7, 20.8.

2,4-toluendiamine:
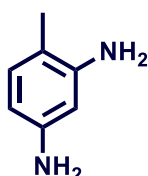
^{1}H NMR (400 MHz, CDCl$_3$) δ 6.82 (d, *J* = 7.8 Hz, 1H), 6.13 – 6.04 (m, 2H), 3.48 (s, 4H), 2.07 (s, 3H).
^{13}C NMR (101 MHz, CDCl3): δ 145.6, 145.4, 131.2, 112.9, 106.0, 102.2, 16.5.
Data are in accordance with literature [10]

4,4'-methylendianiline:
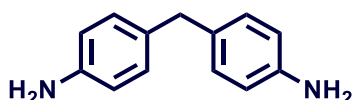
^{1}H NMR (400 MHz, CDCl$_3$) δ 7.01 – 6.91 (m, 4H), 6.66 – 6.57 (m, 4H), 3.77 (s, 2H), 3.54 (s, 4H)
^{13}C NMR (101 MHz, CDCl3): δ 144.4, 132.1, 129.7, 115.4, 40.3

Data are in accordance with literature [10]
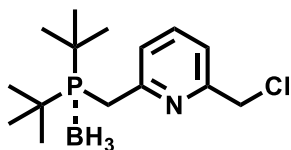
^{1}H NMR (400 MHz, CDCl$_3$) δ 7.64 (t, *J* = 7.7 Hz, 1H), 7.55 (d, *J* = 7.9 Hz, 1H), 7.29 (d, *J* = 7.6 Hz, 3H), 4.60 (s, 2H), 3.35 (d, *J* = 12.2 Hz, 2H), 1.26 (d, *J* = 12.7 Hz, 17H).

Data are in accordance with literature [47]
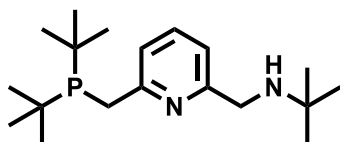
^{1}H NMR (400 MHz, CDCl$_3$) δ 7.51 (t, *J* = 7.9 Hz, 1H), 7.29 (s, 1H), 7.08 (d, *J* = 7.5 Hz, 1H), 3.83 (s, 1H), 3.03 (d, *J* = 3.4 Hz, 1H).

^{31}P NMR (162 MHz, CDCl$_3$) δ 36.1 (s)

Data are in accordance with literature [47]
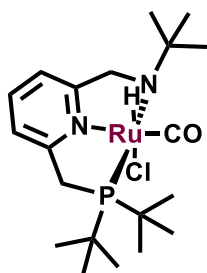
^{1}H NMR (400 MHz, CDCl$_3$) δ 7.58 (t, *J* = 7.8 Hz, 1H), 7.52 (s, 1H), 7.33 (s, 1H), 7.30 (s, 1H), 7.10 (d, *J* = 8.0 Hz, 1H), 4.40 (d, *J* = 14.9 Hz, 2H), 4.21 – 4.02 (m, 1H), 3.73 (dd, *J* = 16.6, 8.1 Hz, 1H), 3.42 (dd, *J* = 16.5, 11.0 Hz, 1H), 1.54 (s, 4H), 1.49 (s, 3H), 1.45 (s, 11H), 1.16 (d, *J* = 13.0 Hz, 8H), - 16.06 (d, *J* = 23.8 Hz, 1H).

^{31}P NMR (162 MHz, CDCl$_3$) δ 109.0 (s).

Data are in accordance with literature [47]

11 MATERIALS AND EQUIPEMENTS:

11.1 GENERAL INFORMATION:

All chemicals were purchased from SigmaAldrich, Fluorochem or Strem Chemicals. THF and DCM were retrieved from a MBraun SP-800 purification system, degassed using argon and stored over 3Å molecular sieves. The remaining solvents were purchased from Sigma-Aldrich or Fluorochem, degassed using argon, stored over 3Å molecular sieves and used without further purification.

Analytical thin layer chromatography (TLC) was performed on silica coated aluminium plates (Merck Kieselgel 60 F254), which were visualized using UV and/or stained with $KMnO_4$ (1.5 g $KMnO_4$ in 1.25 mL NaOH and 200 mL H_2O). Flash column chromatography was performed on silica gel (230-400 mesh).

NMR experiments were performed on a Bruker Ascend 400 spectrometer, where ^{1}H-NMR, ^{13}C-NMR and ^{31}P-NMR were recorded at 400 MHz, 101 MHz and 161.9 MHz, respectively. Abbreviations of multiplicity patterns are given as follows: s = singlet, bs = broad singlet, br. t = broad triplet, d = doublet, t = triplet, q = quartet, quin = quintet, sext = sextet, sep = septet, m = multiplet, dd = double doublet, dt = double triplet, ddd = double double doublet.

IR spectra were measured with a Bruker ALPHA II FT-IR spectrometer and processed with OPUS (release 8.7)

11.2 DESCRIPTION OF AUTOCLAVES:

For all experiments 45 mL pressure vessels were used. The head consists of a single inlet/outlet valve fitted for 5000 Multi Reactor System (Parr®), thermowell for thermocouple insertion, removable PTFE gasket and six stainless steel bolts for sealing the contents of the reaction well. All reactions were set up using a 30 mL PTFE inlay along with fitted magnet. They were heated in aluminium block specially designed to fit the vessels.
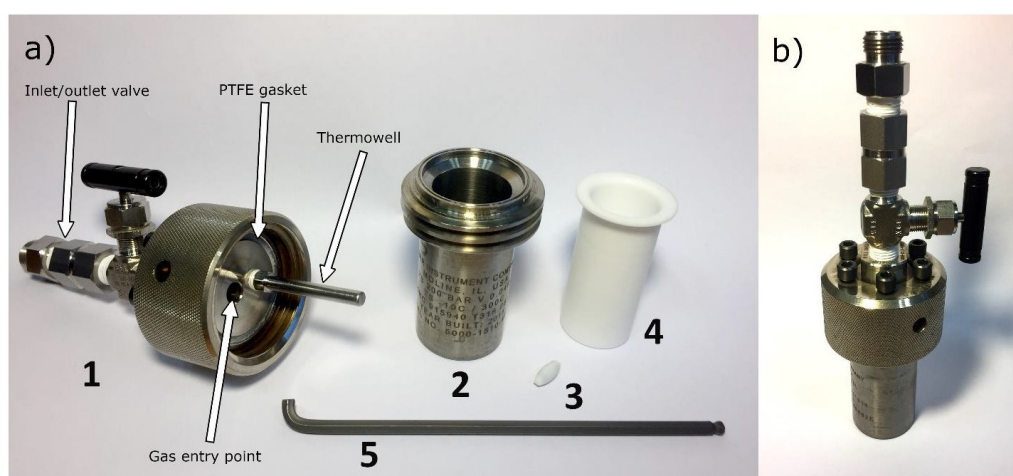
a) Parts of a pressure vessel: 1 - vessel head, 2 - 45 mL reaction well, 3 - magnetic stirring bar, 4 - 30 mL PTFE inlay, 5 - hex key for fastening bolts;
b) Assembled pressure vessel.

11.3 CO-TUBE REACTOR

For the synthesis of ^{iPr}PNN ligand and Ru^{iPr}PNN catalyst 10 mL COtubes were utilized. They were sealed with PTFE/silicon seals purchased from SyTracks as reaction vessel, a Teflon-coated stirring bar and utilized with degassed solvents.

10 mL COtube with screw cap, Teflon disc and septum.

12 SPECTRA:

¹H NMR , ¹³C NMR and FT-IR

2,4 – toluendiame:
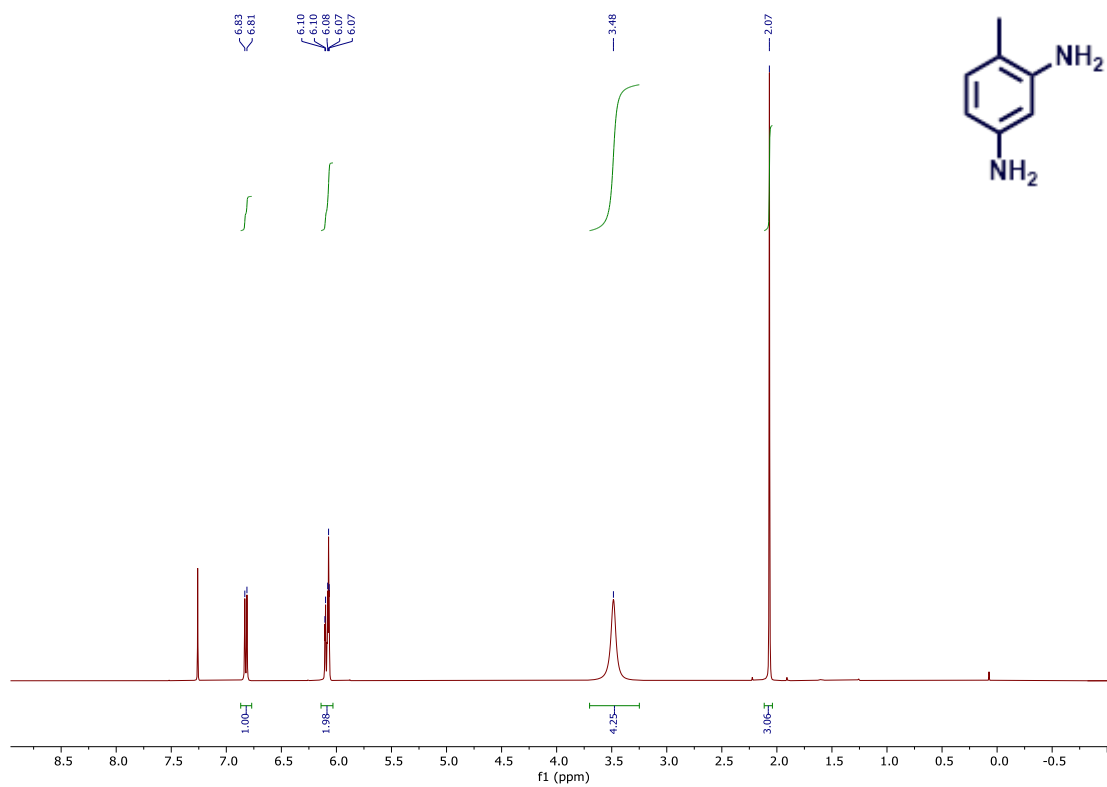
4,4-methylendianiline:
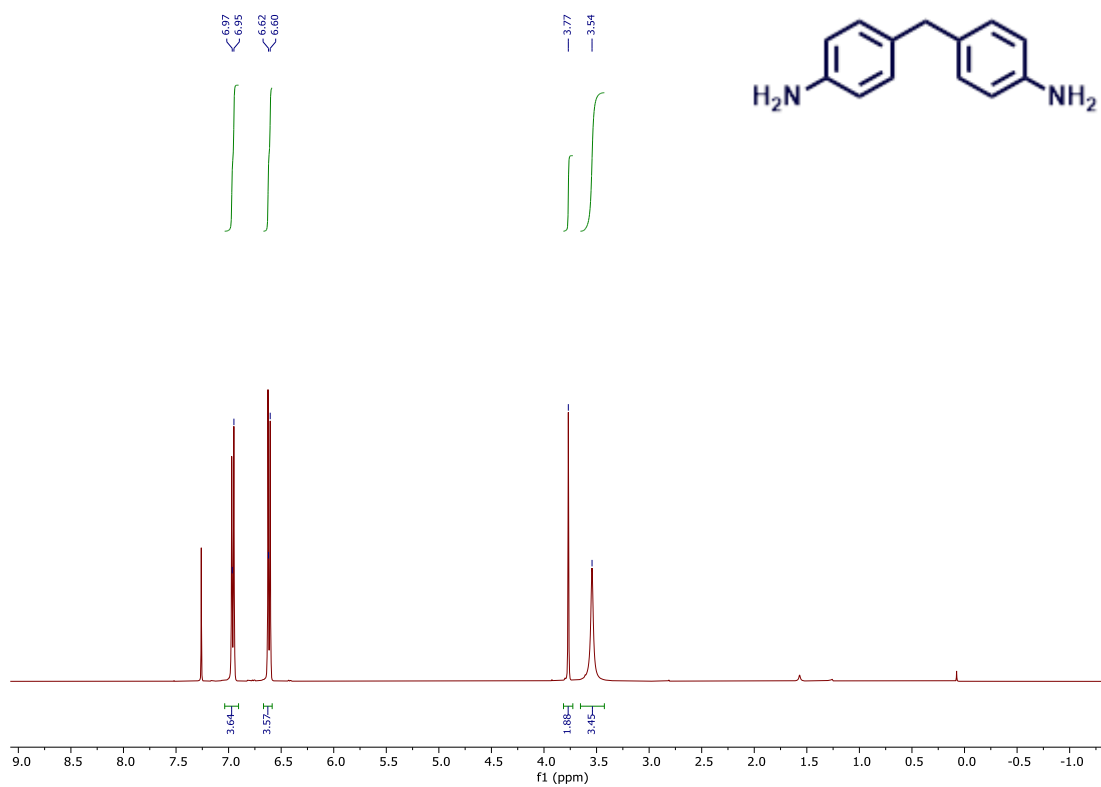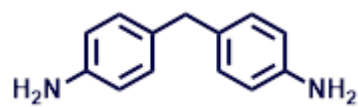
Model 1:
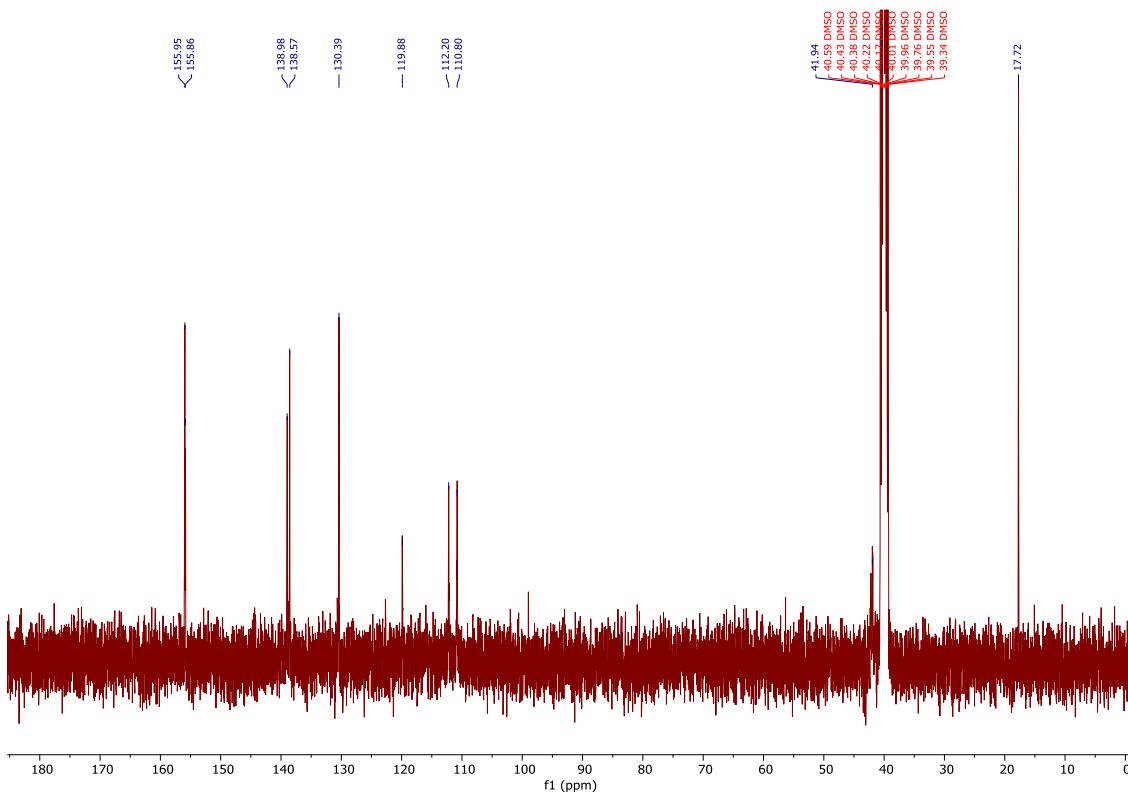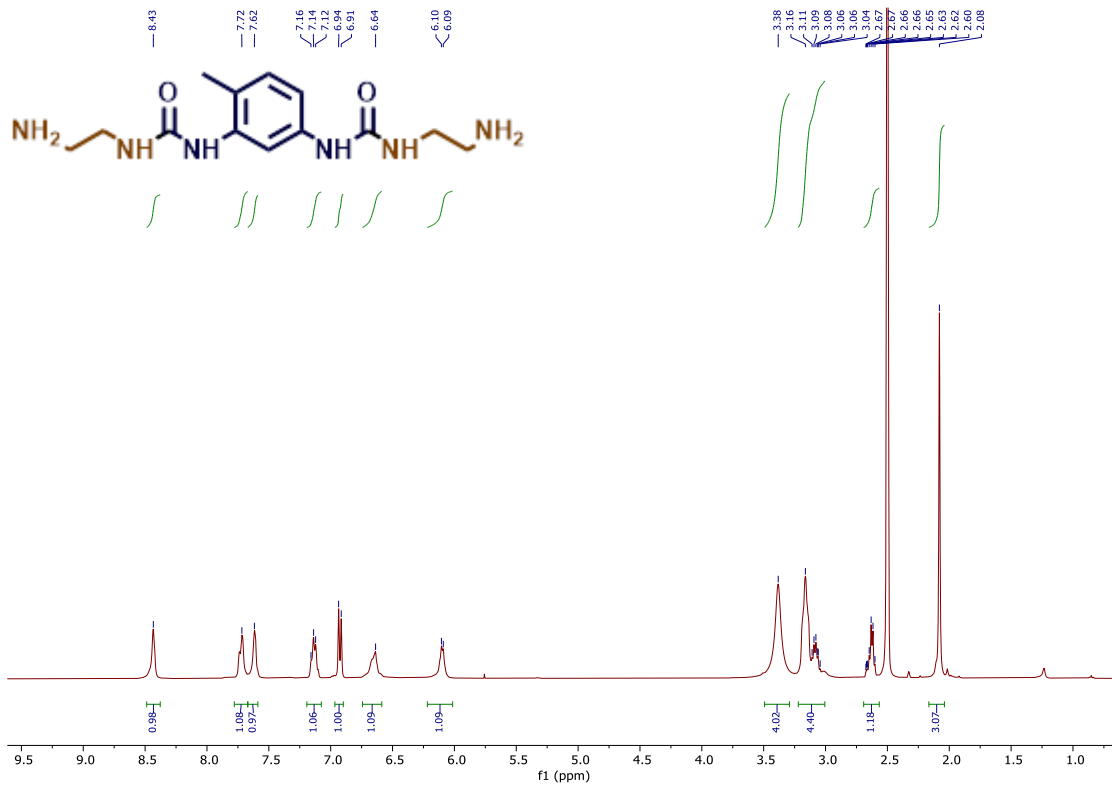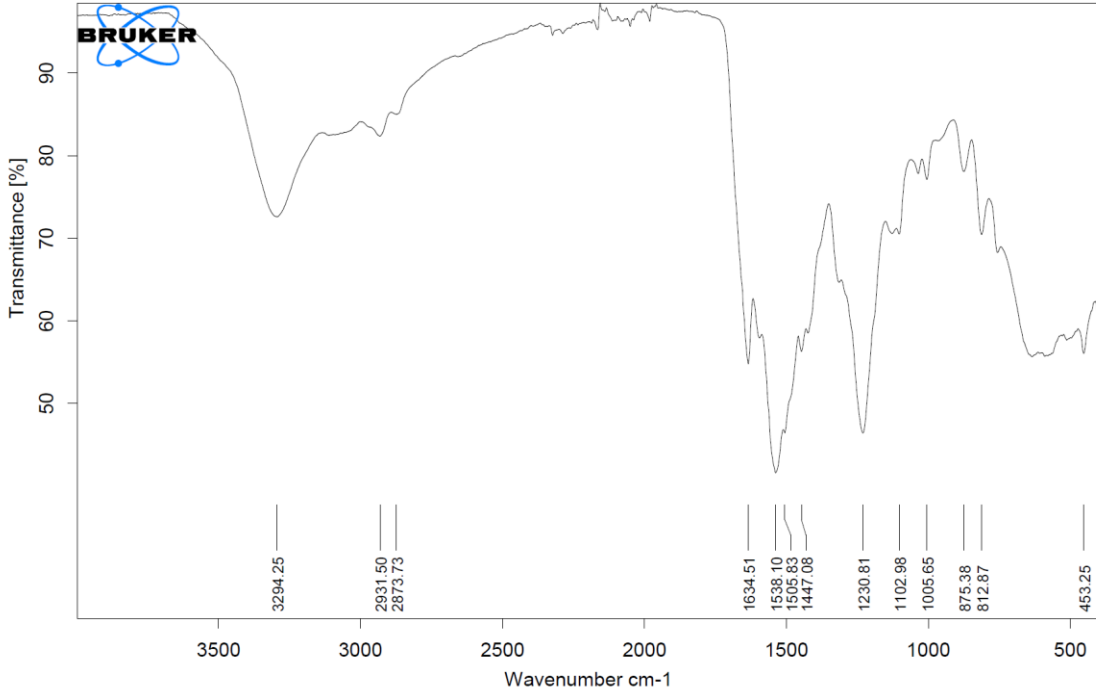
Model 2:
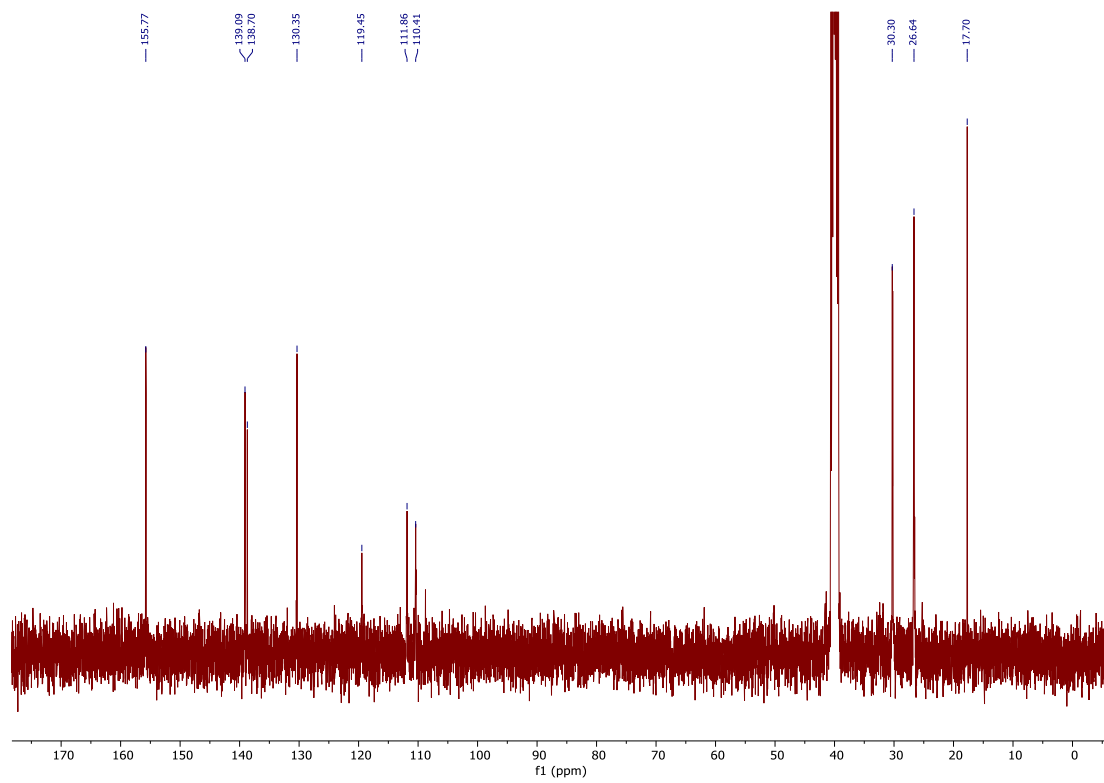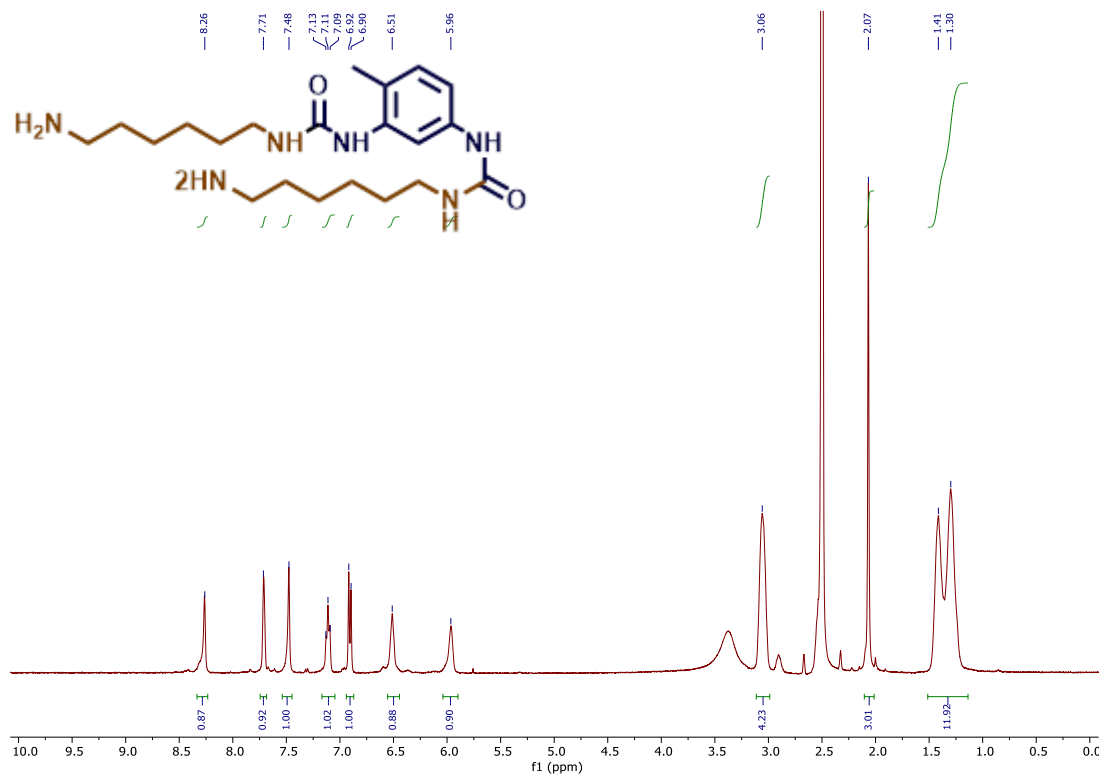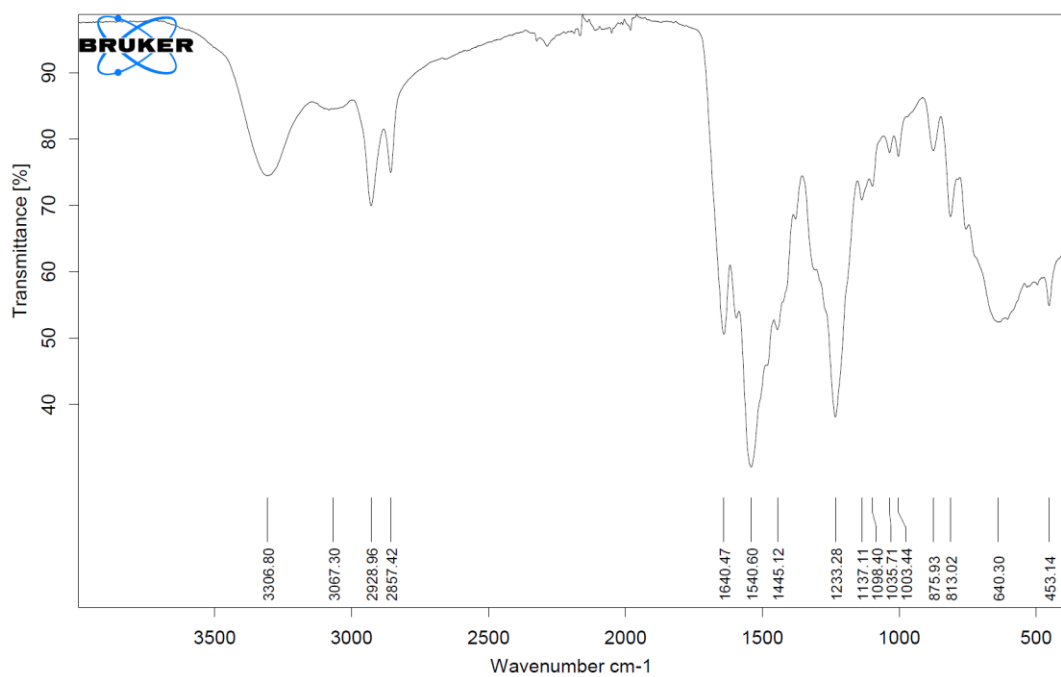
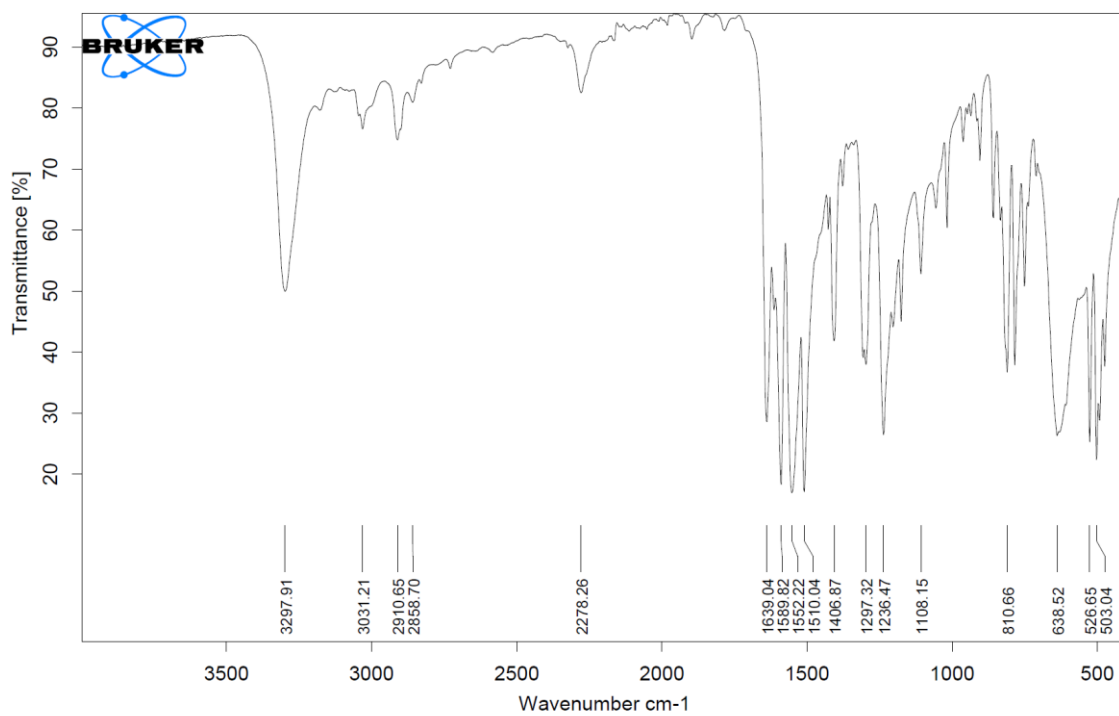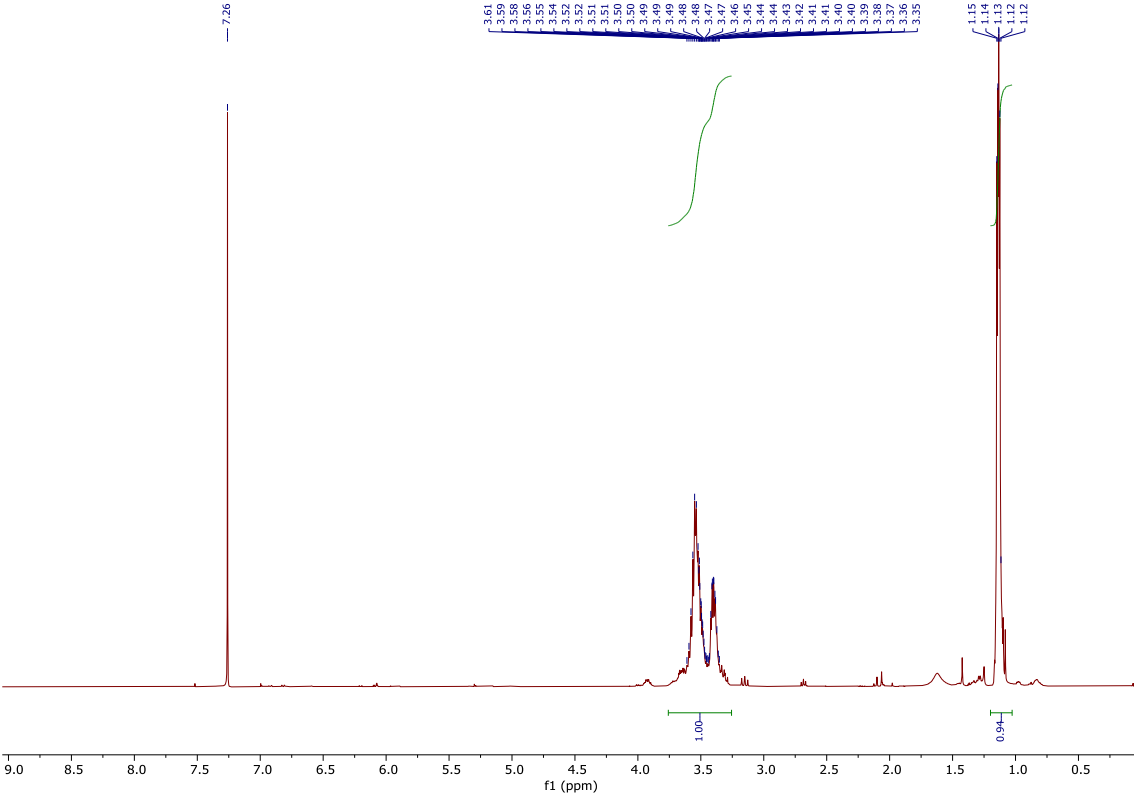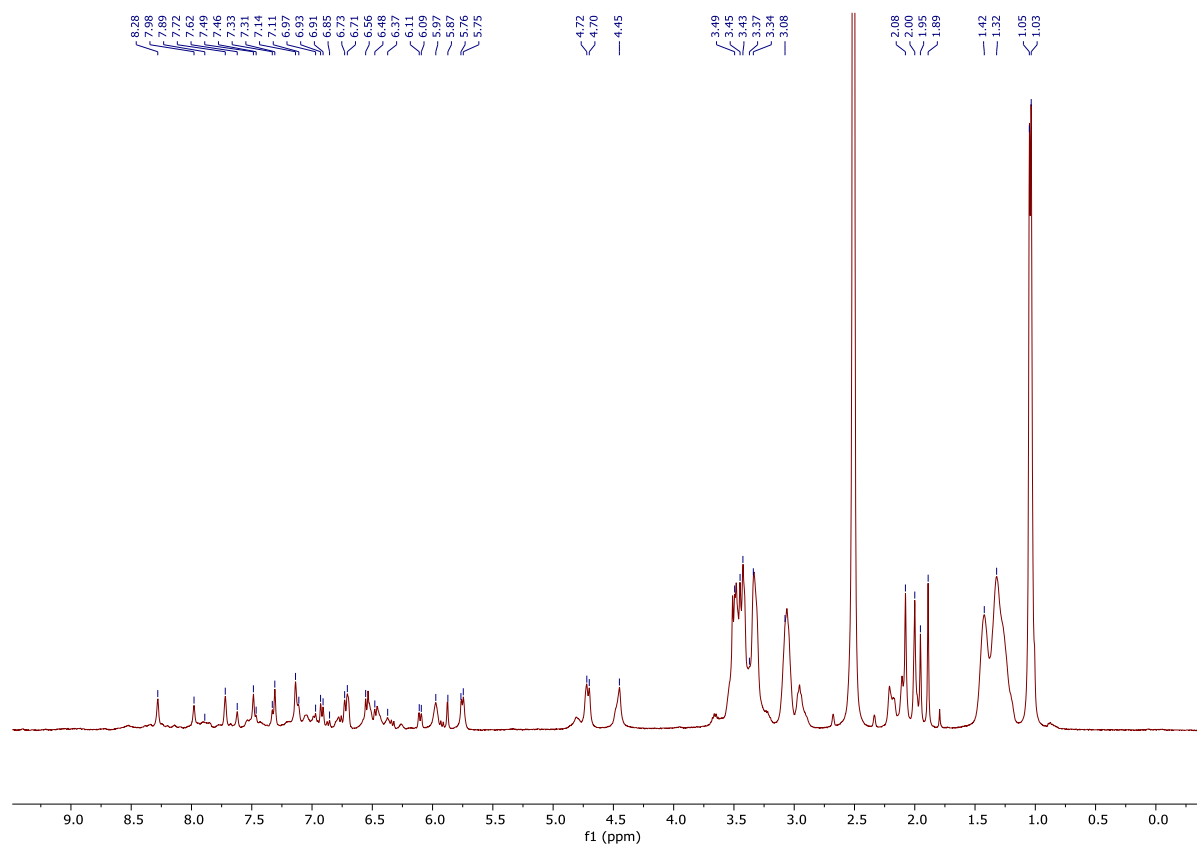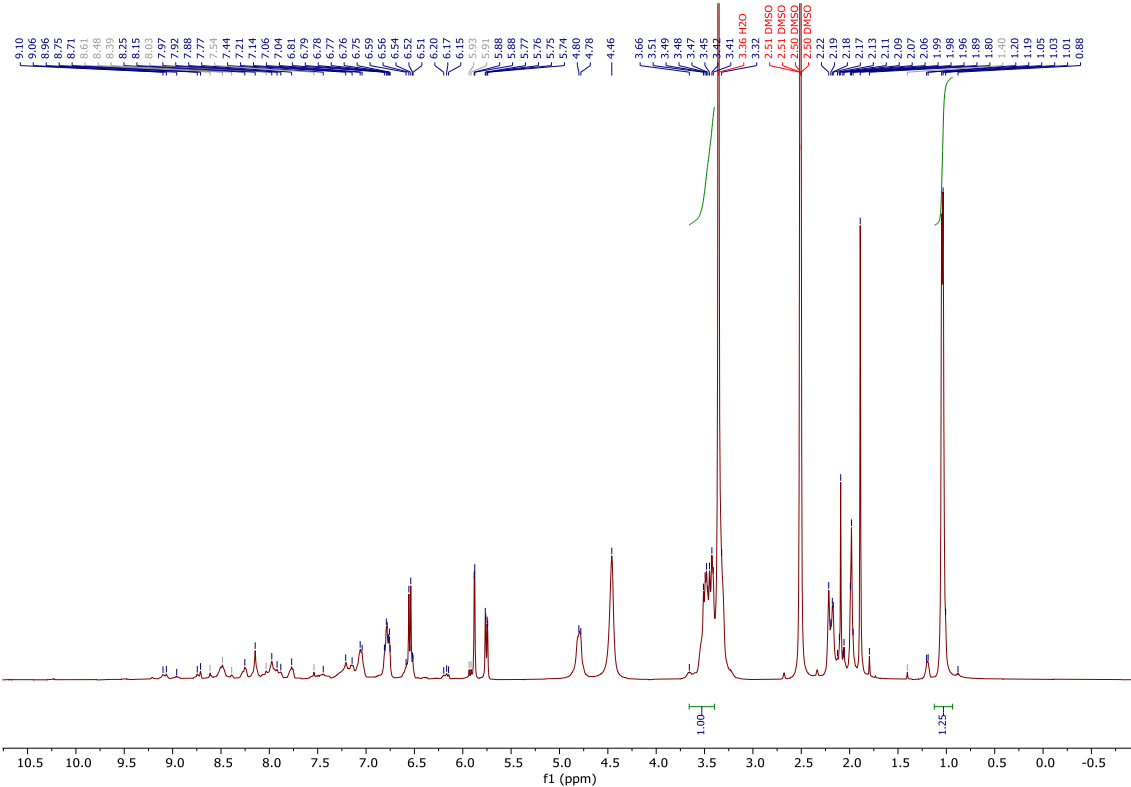**Model 3:**
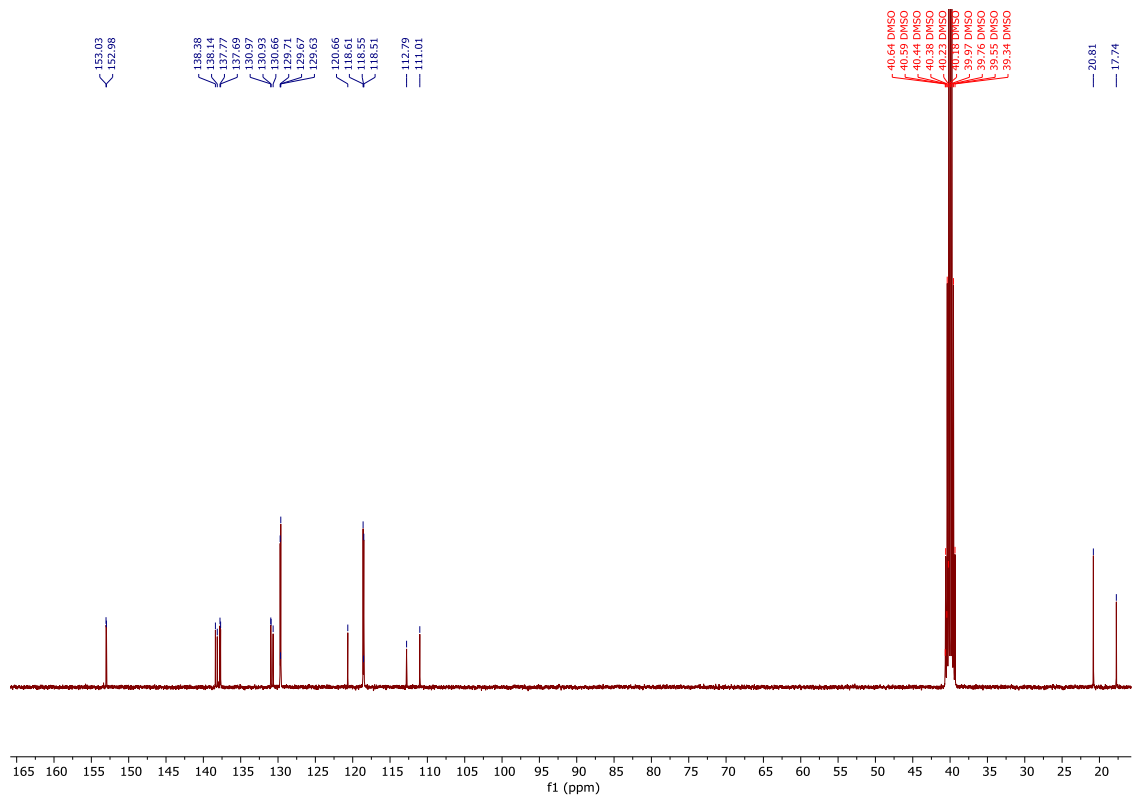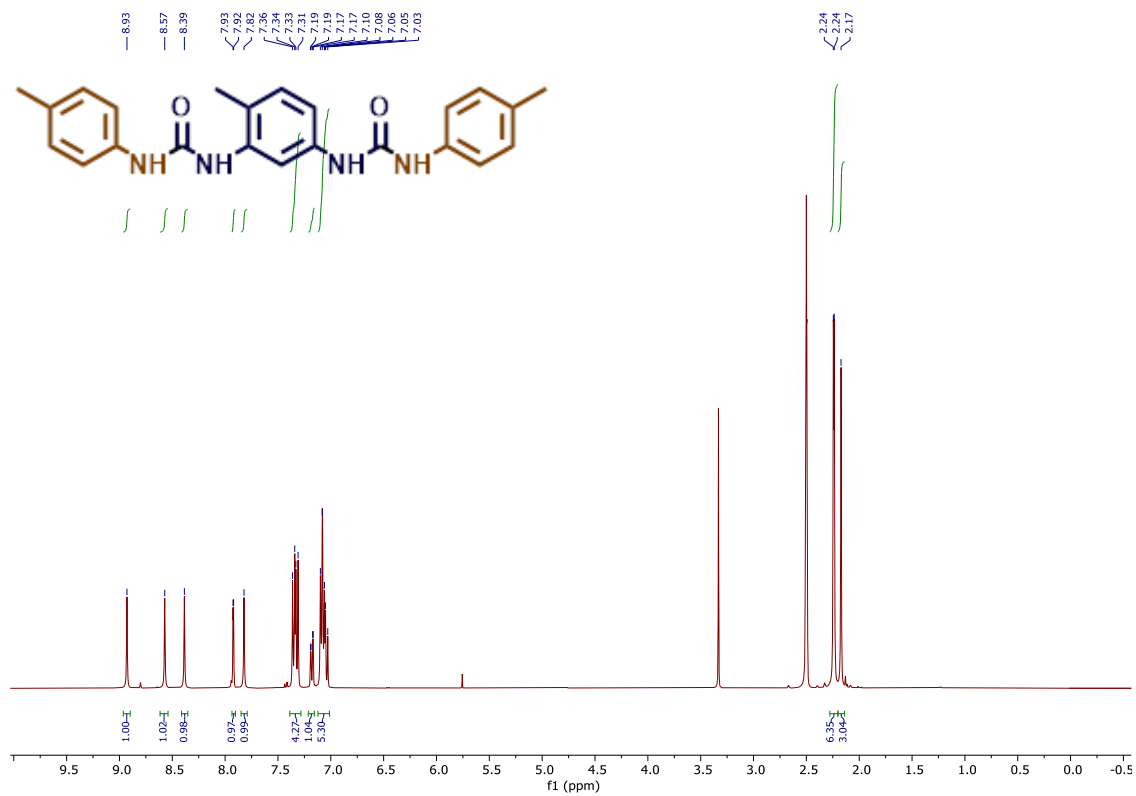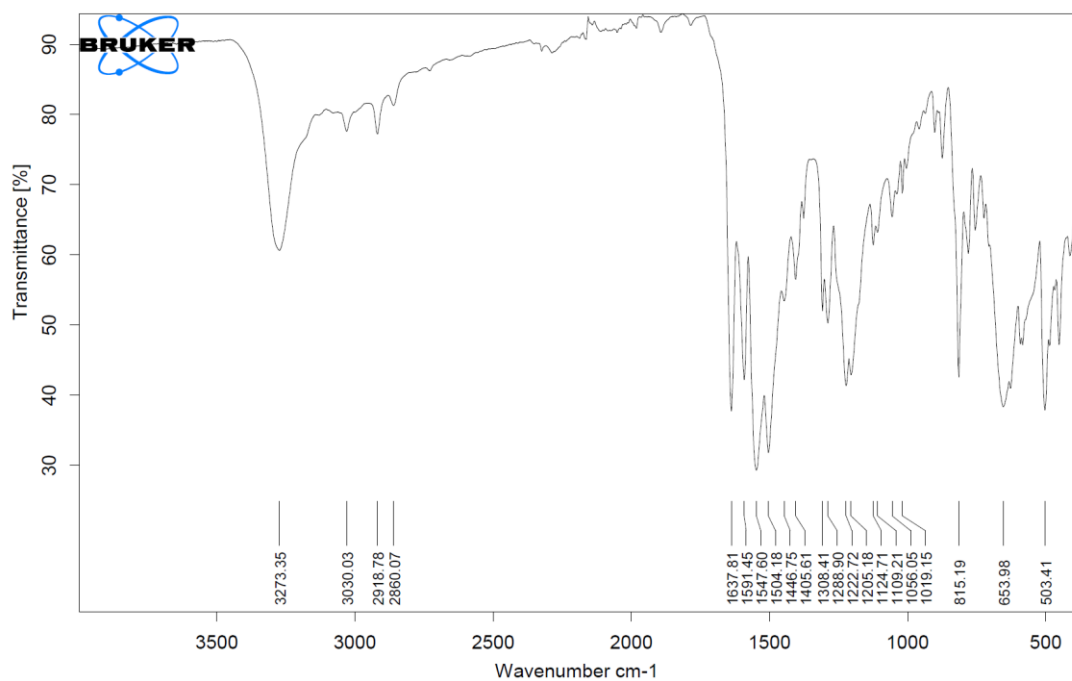
Model 4:
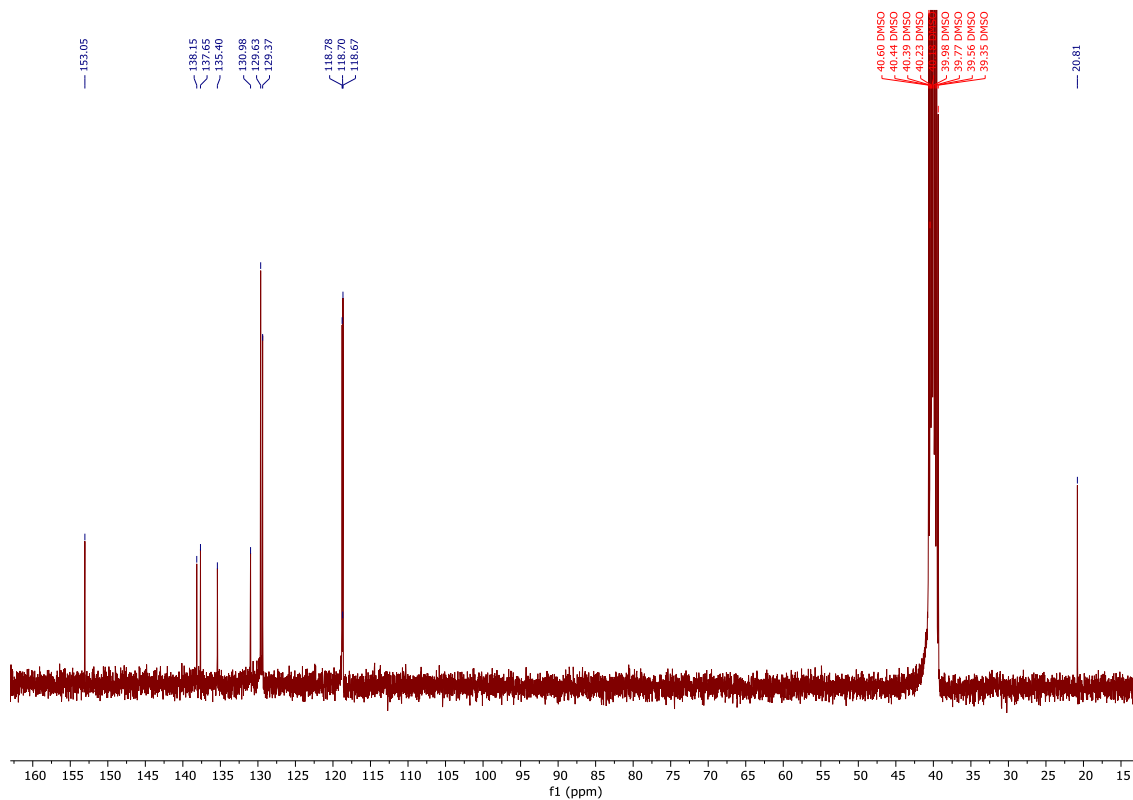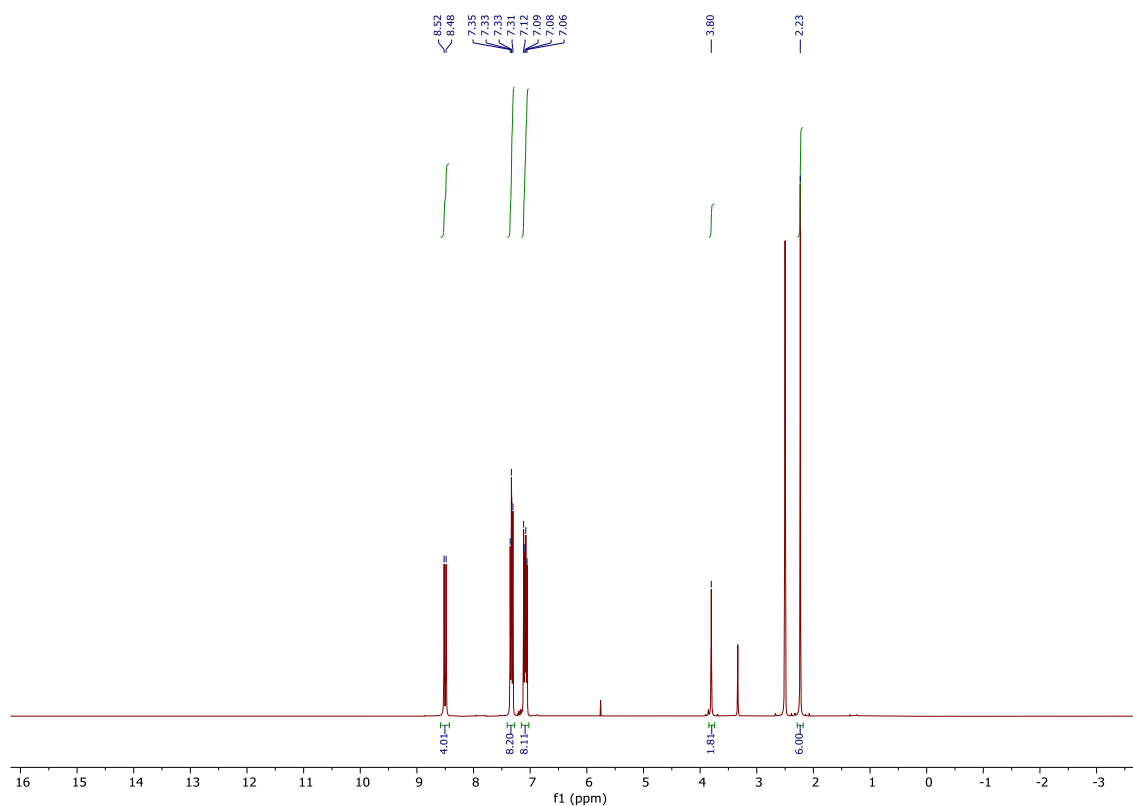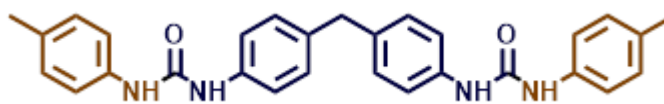
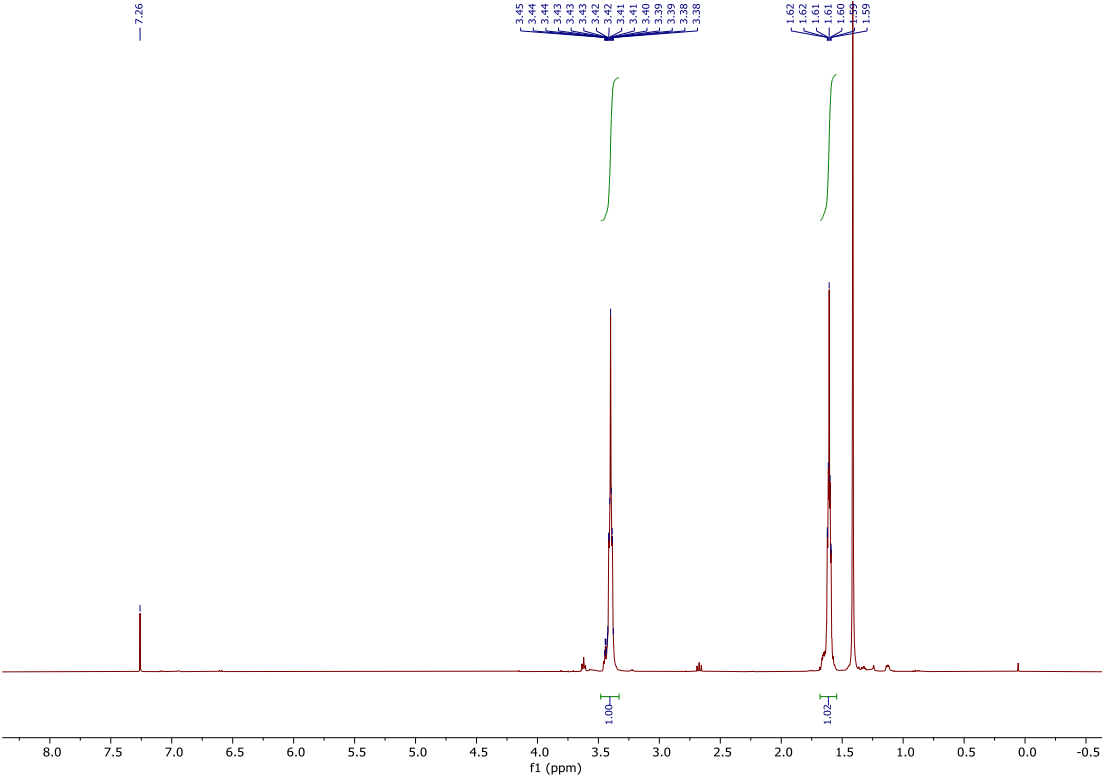Polyol from aminolysis of mattress foam:

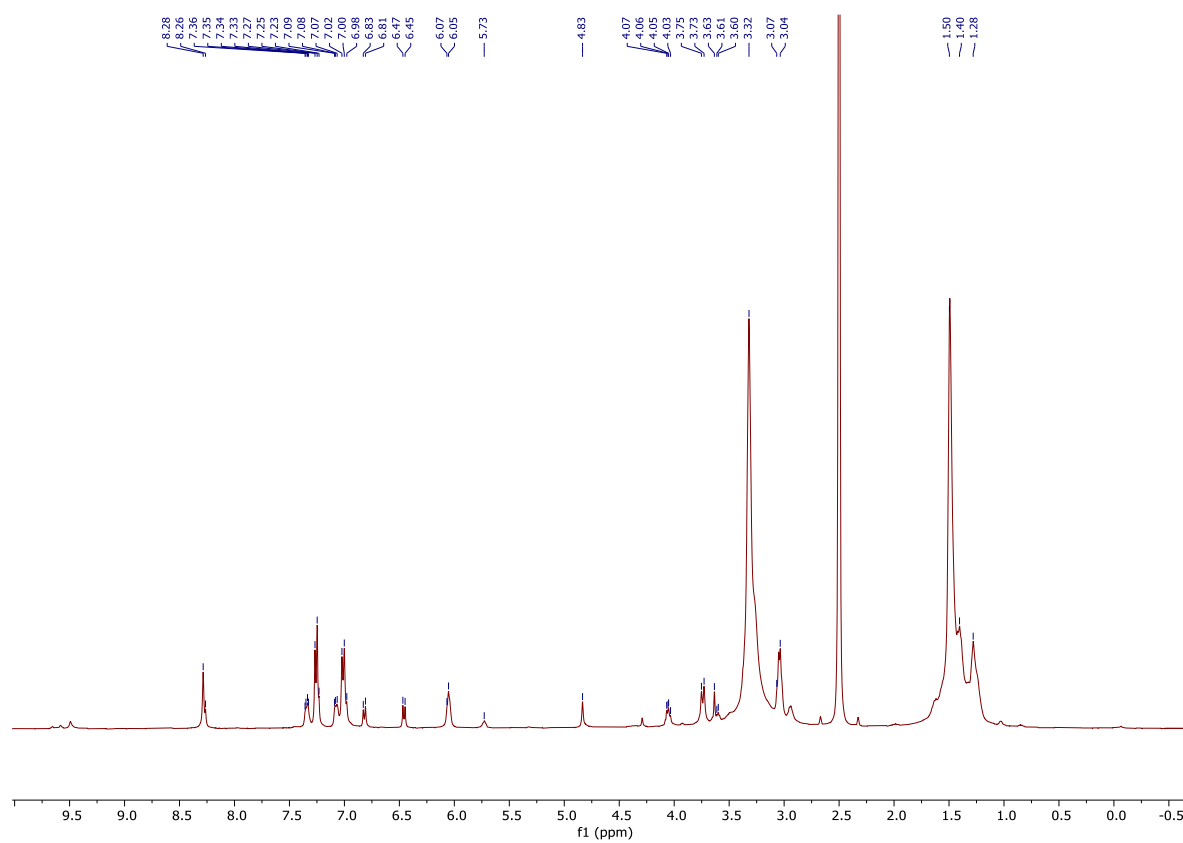Hard segment from aminolysis of mattress foam with hexamethylene diamine:

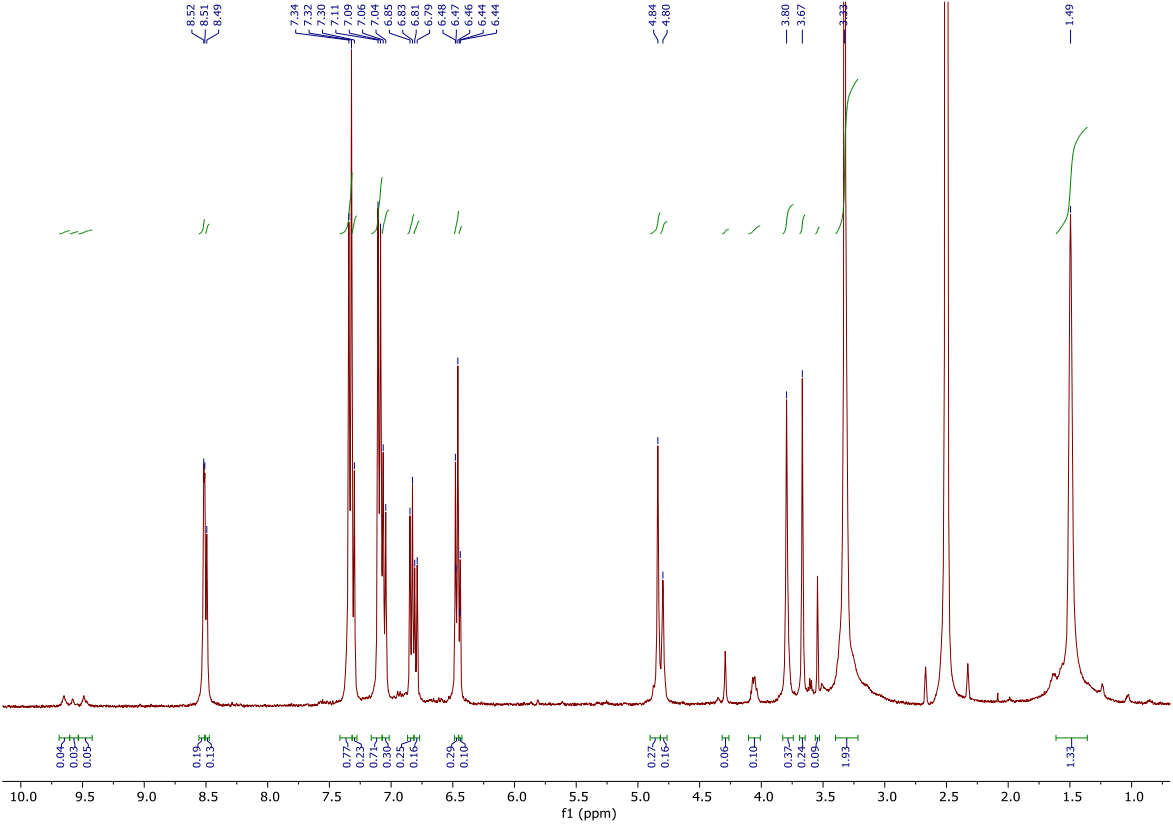Hard segment from aminolysis of mattress foam with 2,4-toluendiamine:
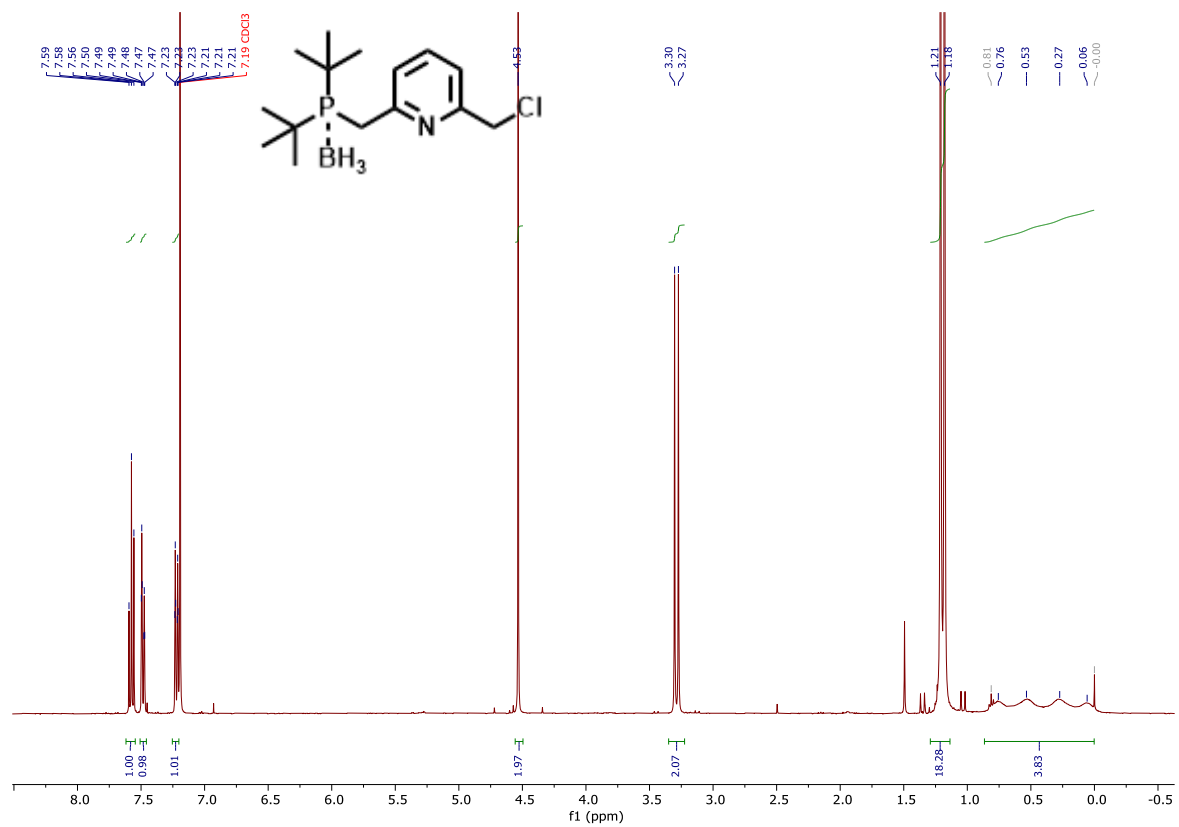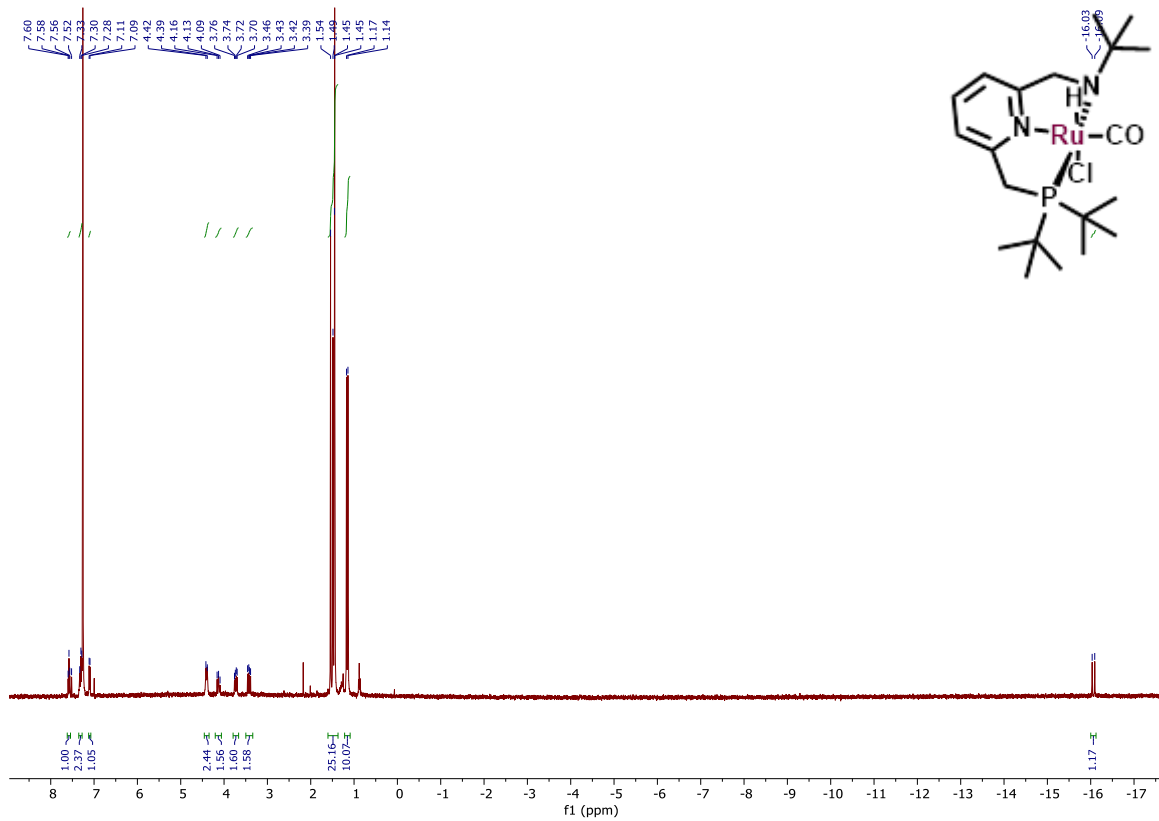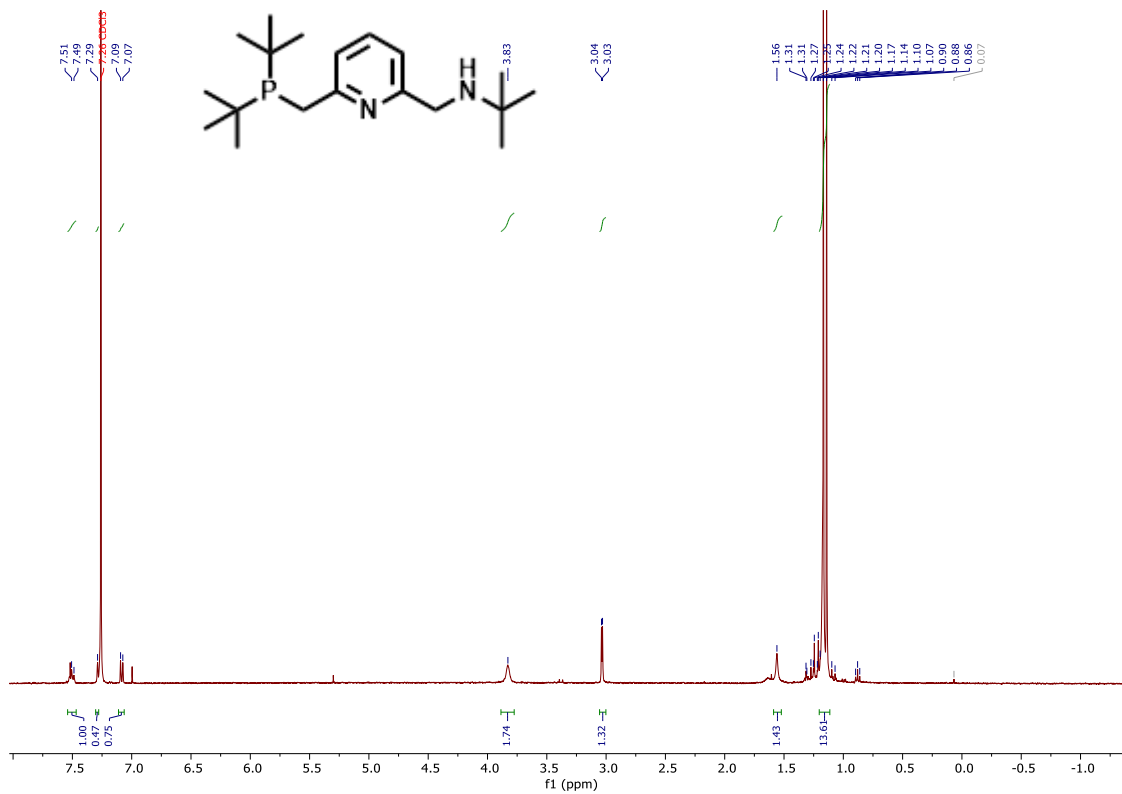
Polyol from aminolysis of shoe foam:

Hard segment from aminolysis of shoe foam with hexamethylene diamine:

Hard segment from aminolysis of shoe foam with 4,4'-methylendianiline:

13 REFERENCES:

(1) Akindoyo, J. O.; Beg, M. D. H.; Ghazali, S.; Islam, M. R.; Jeyaratnam, N.; Yuvaraj, A. R. Polyurethane types, synthesis and applications – a review. *RSC Advances* **2016**, *6* (115).

(2) Engels, H. W.; Pirkl, H. G.; Albers, R.; Albach, R. W.; Krause, J.; Hoffmann, A.; Casselmann, H.; Dormish, J. Polyurethanes: versatile materials and sustainable problem solvers for today's challenges. *Angew Chem Int Ed Engl* **2013**, *52* (36), 9422-9441.

(3) Furtwengler, P.; Avérous, L. Renewable polyols for advanced polyurethane foams from diverse biomass resources. *Polymer Chemistry* **2018**, *9* (32), 4258-4287.

(4) Chattopadhyay, D. K.; Raju, K. V. S. N. Structural engineering of polyurethane coatings for high performance applications. *Progress in Polymer Science* **2007**, *32* (3), 352-418.

(5) Niesiobędzka, J.; Datta, J. Challenges and recent advances in bio-based isocyanate production. *Green Chemistry* **2023**, *25* (7), 2482-2504.

(6) Wittcot, H. A. R., B. G.; Plotkin, J. S. Dinitrotoluene and toluene diisocyante. In *Industrial Organic Chemicals*, 3rd ed.; Wiley, 2013; pp 378-380.

(7) Tran, M. H.; Lee, E. Y. Production of polyols and polyurethane from biomass: a review. *Environmental Chemistry Letters* **2023**, *21* (4), 2199-2223.

(8) Market volume of polyurethane worldwide from 2015 to 2022, with a forecast for 2023 to 2030 (in million metric tons). Statista: 2023; Vol. 2023.

(9) Kemona, A.; Piotrowska, M. Polyurethane Recycling and Disposal: Methods and Prospects. In *Polymers*, 2020; Vol. 12.

(10) Gausas, L.; Kristensen, S. K.; Sun, H.; Ahrens, A.; Donslund, B. S.; Lindhardt, A. T.; Skrydstrup, T. Catalytic Hydrogenation of Polyurethanes to Base Chemicals: From Model Systems to Commercial and End-of-Life Polyurethane Materials. *JACS Au* **2021**, *1* (4), 517-524.

(11) Johansen, M. B.; Donslund, B. S.; Kristensen, S. K.; Lindhardt, A. T.; Skrydstrup, T. tert-Amyl Alcohol-Mediated Deconstruction of Polyurethane for Polyol and Aniline Recovery. *ACS Sustainable Chemistry & Engineering* **2022**, *10* (34), 11191-11202.

(12) Mahoney, L. R.; Weiner, S. A.; Ferris, F. C. Hydrolysis of polyurethane foam waste. *Environmental Science & Technology* **1974**, *8* (2), 135-139.

(13) Heiran, R.; Ghaderian, A.; Reghunadhan, A.; Sedaghati, F.; Thomas, S.; Haghighi, A. h. Glycolysis: an efficient route for recycling of end of life polyurethane foams. *Journal of Polymer Research* **2021**, *28* (1), 22.

(14) Zubar, V.; Haedler, A. T.; Schütte, M.; Hashmi, A. S. K.; Schaub, T. Hydrogenative Depolymerization of Polyurethanes Catalyzed by a Manganese Pincer Complex. *ChemSusChem* **2022**, *15* (1).

(15) Kumar, A.; von Wolff, N.; Rauch, M.; Zou, Y.-Q.; Shmul, G.; Ben-David, Y.; Leitus, G.; Avram, L.; Milstein, D. Hydrogenative Depolymerization of Nylons. *Journal of the American Chemical Society* **2020**, *142* (33).

(16) Gausas, L.; Donslund, B. S.; Kristensen, S. K.; Skrydstrup, T. Evaluation of Manganese Catalysts for the Hydrogenative Deconstruction of Commercial and End-of-Life Polyurethane Samples. *ChemSusChem* **2022**, *15* (1).

(17) Grdadolnik, M.; Drinčić, A.; Oreški, A.; Onder, O. C.; Utroša, P.; Pahovnik, D.; Žagar, E. Insight into Chemical Recycling of Flexible Polyurethane Foams by Acidolysis. *ACS Sustainable Chemistry & Engineering* **2022**, *10* (3).

(18) Grdadolnik, M.; Zdovc, B.; Drinčić, A.; Onder, O. C.; Utroša, P.; Ramos, S. G.; Ramos, E. D.; Pahovnik, D.; Žagar, E. Chemical Recycling of Flexible Polyurethane Foams by Aminolysis to Recover High-Quality Polyols. *ACS Sustainable Chemistry & Engineering* **2023**, *11* (29).

(19) Zhang, Q.; Wang, S.; Rao, B.; Chen, X.; Ma, L.; Cui, C.; Zhong, Q.; Li, Z.; Cheng, Y.; Zhang, Y. Hindered urea bonds for dynamic polymers: An overview. *Reactive and Functional Polymers* **2021**, *159*.

(20) Ying, H.; Zhang, Y.; Cheng, J. Dynamic urea bond for the design of reversible and self-healing polymers. *Nature Communications* **2014**, *5* (1), 3218.

(21) Hutchby, M.; Houlden, C. E.; Ford, J. G.; Tyler, S. N. G.; Gagné, M. R.; Lloyd-Jones, G. C.; Booker-Milburn, K. I. Hindered Ureas as Masked Isocyanates: Facile Carbamoylation of Nucleophiles under Neutral Conditions. *Angewandte Chemie International Edition* **2009**, *48* (46), 8721-8724.

(22) Ying, H.; Cheng, J. Hydrolyzable Polyureas Bearing Hindered Urea Bonds. *Journal of the American Chemical Society* **2014**, *136* (49), 16974-16977.

(23) Liu, M.; Wang, Y.; Wu, Y.; Wan, H. Hydrolysis and recycling of urea formaldehyde resin residues. *Journal of Hazardous Materials* **2018**, *355*, 96-103.

(24) Medina-Ramos, W.; Mojica, M. A.; Cope, E. D.; Hart, R. J.; Pollet, P.; Eckert, C. A.; Liotta, C. L. Water at elevated temperatures (WET): reactant, catalyst, and solvent in the selective hydrolysis of protecting groups. *Green Chemistry* **2014**, *16* (4), 2147-2155.

(25) Savage, P. E. A perspective on catalysis in sub- and supercritical water. *The Journal of Supercritical Fluids* **2009**, *47* (3), 407-414.

(26) Cabrero-Antonino, J. R.; Adam, R.; Papa, V.; Beller, M. Homogeneous and heterogeneous catalytic reduction of amides and related compounds using molecular hydrogen. *Nature Communications* **2020**, *11* (1), 3893.

(27) Das, U. K.; Kumar, A.; Ben-David, Y.; Iron, M. A.; Milstein, D. Manganese Catalyzed Hydrogenation of Carbamates and Urea Derivatives. *Journal of the American Chemical Society* **2019**, *141* (33), 12962-12966.

(28) Gunanathan, C.; Milstein, D. Metal–Ligand Cooperation by Aromatization–Dearomatization: A New Paradigm in Bond Activation and "Green" Catalysis. *Accounts of Chemical Research* **2011**, *44* (8), 588-602.

(29) Balaraman, E.; Ben-David, Y.; Milstein, D. Unprecedented catalytic hydrogenation of urea derivatives to amines and methanol. *Angew Chem Int Ed Engl* **2011**, *50* (49), 11702-11705.

(30) Milstein, D.; Hu, P.; Fogler, E.; Rao, J. A. G. N. Ruthenium complexes and their uses as catalysts in processes for formation and/or hydrogenation of esters, amides and related reactions. Google Patents: 2020.

(31) Milstein, D. Discovery of Environmentally Benign Catalytic Reactions of Alcohols Catalyzed by Pyridine-Based Pincer Ru Complexes, Based on Metal–Ligand Cooperation. *Topics in Catalysis* **2010**, *53* (13), 915-923.

(32) Amit Kumar, J. L. Catalytic Hydrogenation of Urea Derivatives and Polyureas. *European Jurnal of Organic Chemistry* **2021**.

(33) Rong, H.; Zhang, Y.; Ai, X.; Li, W.; Cao, F.; Li, L. Theoretical Study on the Hydrogenolysis of Polyurethanes to Improve the Catalytic Activities. *Inorganic Chemistry* **2022**, *61* (37), 14662-14672.

(34) Liu, X.; Werner, T. Indirect reduction of CO_2 and recycling of polymers by manganese-catalyzed transfer hydrogenation of amides, carbamates, urea derivatives, and polyurethanes. *Chemical Science* **2021**, *12* (31), 10590-10597, 10.1039/D1SC02663A.

(35) Dyson, P. J.; Jessop, P. G. Solvent effects in catalysis: rational improvements of catalysts via manipulation of solvent interactions. *Catalysis Science & Technology* **2016**, *6* (10), 3302-3316.

(36) Johansen, M. B.; Donslund, B. S.; Kristensen, S. K.; Lindhardt, A. T.; Skrydstrup, T. *tert*-Amyl Alcohol-Mediated Deconstruction of Polyurethane for Polyol

and Aniline Recovery. *ACS Sustainable Chemistry & Engineering* **2022**, *10* (34), 11191-11202.

(37) Grdadolnik, M.; Zdovc, B.; Drinčić, A.; Onder, O. C.; Utroša, P.; Ramos, S. G.; Ramos, E. D.; Pahovnik, D.; Žagar, E. Chemical Recycling of Flexible Polyurethane Foams by Aminolysis to Recover High-Quality Polyols. *ACS Sustainable Chemistry & Engineering* **2023**.

(38) Olazabal, I.; González, A.; Vallejos, S.; Rivilla, I.; Jehanno, C.; Sardon, H. Upgrading Polyurethanes into Functional Ureas through the Asymmetric Chemical Deconstruction of Carbamates. *ACS Sustainable Chemistry & Engineering* **2023**, *11* (1), 332-342.

(39) Bhandari, S.; Gupta, P. 7 - Chemical Depolymerization of Polyurethane Foam via Ammonolysis and Aminolysis. In *Recycling of Polyurethane Foams*, Thomas, S., Rane, A. V., Kanny, K., V.K, A., Thomas, M. G. Eds.; William Andrew Publishing, 2018; pp 77-87.

(40) Neofotistos, S. P.; Tzani, A.; Detsi, A. Ionic Liquids: Advances and Applications in Phase Transfer Catalysis. In *Catalysts*, 2023; Vol. 13.
(41) Ponomareva, V. G.; Bagryantseva, I. N.; Uvarov, N. F. Electrotransport and thermal properties of tetrabutylammonium hydrogen sulfate. *Ionics* **2021**, *27* (5), 2067-2071.
(42) Deguchi, Y.; Kono, M.; Koizumi, Y.; Izato, Y.-i.; Miyake, A. Study on Autocatalytic Decomposition of Dimethyl Sulfoxide (DMSO). *Organic Process Research & Development* **2020**, *24* (9), 1614-1620.

(43) Alfonsi, K.; Colberg, J.; Dunn, P. J.; Fevig, T.; Jennings, S.; Johnson, T. A.; Kleine, H. P.; Knight, C.; Nagy, M. A.; Perry, D. A.; et al. Green chemistry tools to influence a medicinal chemistry and research chemistry based organisation. *Green Chemistry* **2008**, *10* (1), 31-36.

(44) Dawe, L. N.; Karimzadeh-Younjali, M.; Dai, Z.; Khaskin, E.; Gusev, D. G. The Milstein Bipyridyl PNN Pincer Complex of Ruthenium Becomes a Noyori-Type Catalyst under Reducing Conditions. *Journal of the American Chemical Society* **2020**, *142* (46), 19510-19522.

(45) Godinho, B.; Gama, N.; Barros-Timmons, A.; Ferreira, A. Recycling of different types of polyurethane foam wastes via acidolysis to produce polyurethane coatings. *Sustainable Materials and Technologies* **2021**, *29*.

(46) Zhang, J.; Leitus, G.; Ben-David, Y.; Milstein, D. Facile Conversion of Alcohols into Esters and Dihydrogen Catalyzed by New Ruthenium Complexes. *Journal of the American Chemical Society* **2005**, *127* (31), 10840-10841.

(47) Holmes, A. J.; Rayner, P. J.; Cowley, M. J.; Green, G. G. R.; Whitwood, A. C.; Duckett, S. B. The reaction of an iridium PNP complex with parahydrogen facilitates

polarisation transfer without chemical change. *Dalton Transactions* **2015**, *44* (3), 1077-1083.